Numerical Modelling of a Macrotidal Bay over the Last 9,000 Years: An Interdisciplinary Methodology to Understand the Influence of Sea-Level Variations on Tidal Currents in the Bay of Brest

Matthieu Guillaume Olivier, Estelle Leroux, Marina Rabineau, Pierre Le Hir, Didier Granjeon, Teddy Chataigner, Alexis Beudin, Heloise Muller

Continental Shelf Research 231 (2021) 104595

Contents lists available at ScienceDirect

Continental Shelf Research

journal homepage: www.elsevier.com/locate/csr

Numerical modelling of a Macrotidal Bay over the last 9,000 years: An interdisciplinary methodology to understand the influence of sea-level variations on tidal currents in the Bay of Brest

Matthieu Guillaume Olivier [a,c,d,*], Estelle Leroux [a], Marina Rabineau [d], Pierre Le Hir [b], Didier Granjeon [c], Teddy Chataigner [e], Alexis Beudin [f], Heloise Muller [b]

[a] IFREMER – LGS laboratory – Pointe du Diable, 29280, Plouzané, France
[b] IFREMER – DYNECO/DHYSED laboratory – Pointe du Diable, 29280, Plouzané, France
[c] IFP Énergies nouvelles – 1 et 4, avenue de Bois-Préau, 92500, Rueil-Malmaison, France
[d] Univ Brest, CNRS, Univ. Bretagne-Sud, Laboratoire Géosciences Océan (LGO), UMR6538, IUEM, rue Dumont d'Urville, F-29280, Plouzané, France
[e] ENPC, Hydraulics Laboratory, Saint-Venant, 6 quai Watier, 78400, Chatou, France
[f] BW-CGC, 53 rue du commandant Groix, 29200, Brest, France

ARTICLE INFO

Keywords:
Hydrodynamic modelling
Tidal currents
Paleoenvironmental reconstruction
Holocene sedimentation
Erosion and deposition potential indexes

ABSTRACT

Estuaries play a major role in the transfer of sediments from the continents to the shelves and deep ocean basins. Their position at the interface between land and sea promotes them as a key area for the understanding of ocean sediment supply, but yet long-term evolution remains poorly understood. The main reasons of the lack of knowledge about estuaries filling are the lack of hydrodynamic data in the past and the temporal application of numerical models. Oceanographers and geologists have developed numerical models to simulate currents and sedimentation. On one hand, hydro-sediment models allow a good physical representation of estuarine hydrodynamic processes and their impact on sedimentation, but only over time-scale spanning years to decades. On the other hand, stratigraphic diffusive models aim to study the impact of various geological processes on sedimentary basins over millions of years, but they are unable to describe in detail the tidal hydrodynamic processes that govern estuaries.

In response to this timescale issue, this study presents a first step attempt to explore the evolution of tidal current distribution in relation with Holocene eustatic variations and seafloor evolution. Here we focus on a macro-tidal estuary, the bay of Brest, where tidal processes dominate, as the estuary is naturally protected from ocean swells. This paper aims to set up a methodology to simulate the (past) tidal currents over a long time period and correlate them with sedimentary data. Major changes in deposit dynamics are first identified from cores and seismic data, and the corresponding paleo-topographies and paleo-sea-levels are rebuilt. A process-based hydrodynamic model (MARS3D) is then used to test the impacts of these paleo-bathymetries on hydrodynamics over a 1-year time span. Four scenarii have been considered, representing four key stages of the Holocene transgression in the Bay of Brest.

The simulated barotropic currents distributions were analysed and bottom currents impact on the seafloor compared with sedimentary records to understand past hydrodynamic context and associated sediment spatial distribution over geological time scale. Hydrodynamic simulations and sediments records are linked, in order to propose a reconstruction of the tidal influence on sediments over the last 9000 years. The results show changes of the tidal patterns related to the paleoenvironmental evolution (bathymetry and sea-level variations). Even if a hydro-sediment model would be needed to make a direct correlation between simulated currents and sediment records, this successful application in the Bay of Brest shows that discontinuous modelling can help to understand tidal current evolution and their impact on sediment distribution over long periods.

* Corresponding author. IFREMER – LGS laboratory – Pointe du Diable, 29280, Plouzané, France.
E-mail addresses: molivier@ifremer.fr (M. Guillaume Olivier), eleroux@ifremer.fr (E. Leroux), marina.rabineau@univ-brest.fr (M. Rabineau), Pierre.Le.Hir@ifremer.fr (P. Le Hir), didier.granjeon@ifpen.fr (D. Granjeon), teddy.chataigner@enpc.fr (T. Chataigner), alexis.beudin@bw-cgc.fr (A. Beudin), hmuller@ifremer.fr (H. Muller).

https://doi.org/10.1016/j.csr.2021.104595
Received 19 March 2021; Received in revised form 8 October 2021; Accepted 14 October 2021
Available online 23 October 2021

1. Introduction

Past estuarine sedimentary systems remain poorly understood, yet they are key areas in the global understanding of sedimentary dynamics. Estuaries are located at the interface between rivers and ocean basins and represent a key link between the source and sink in a source-to-sink approach. As complex and always changing environments, for example regarding their salinity characteristics, they host a specific type of biodiversity. The very heterogeneous petrophysical properties of tidal sedimentary rocks in these environments, the abundance of life, organic matter and specific morphology such as incised valleys can make them excellent petroleum systems (Posamentier and Allen, 1993; Dalrymple, 2010). Besides the resource aspect, within the context of Holocene deglaciation and sea-level rise, the action of tidal currents is expected to change significantly along and over the coastline. Understanding the influence of the sea-level and the bathymetry on tides over a rather long period of time (9 ka) is therefore important in both past and future contexts. It appears that there are mainly two ways to explore changes in tidal circulation: a detailed study of the sedimentary record, which is an indirect approach, or numerical modelling. This last option is vast, as several types of modelling are available to study geomorphological changes in coastal areas.

For geological timescales (more than 1 Ka), stratigraphic models are the most popular. Stratigraphic models use a deterministic approach based on diffusion, which is the only approach allowing the simulation of the filling of sedimentary basins at the time and space scales considered in geology. They aim to simulate the synthetic result of geological processes over millions of years (Granjeon and Joseph, 1999; Bruneau et al., 2017; Crombez et al., 2017). They deal with the results of long-term processes such as subsidence or tectonic movements and, as they are not based on high resolution processes, their computational costs are rather small. Thus, due to the high frequency oscillations of tidal processes, stratigraphic models do not consider explicitly tidal processes and at present-day, they are unable to simulate the residual effect of tides over long time periods.

On another side, oceanographers have developed hydrodynamic and hydro-sediment models based on the resolution of physical processes, which allow to study the hydrodynamic effects on sedimentation at very fine spatial scale (meter), but only over short-time periods (from hours to decades, e.g. Bárcena et al., 2016; Grasso and Le Hir, 2019; Tosic et al., 2019). As they are based on the physical representation of processes that evolve rapidly (wind-induced and tidal currents, wave regimes, density-induced flows, erosion, deposition, bedload or suspended sediment transport), the calculation steps are very short (~10 s). The computational time of hydro-sediment models doesn't allow to simulate periods longer than 10 years, unless simplifications of the integration of the time-consuming processes are made. In Cayocca (2000) for example, tidal currents computation is simplified (annual mean) to simulate the last 300 years of the coastal evolution of Arcachon lagoon. The morphological evolutions of nearshore basins are most often approached by the so-called "reduced complexity models". It is an important topic for society but complex for researchers, because it mixes processes in the order of 1 s with others in the order of one hundred years. Many techniques have been developed to simulate this type of environment, a synthesis of these techniques is proposed by Roelvink (2006). The most used technique is to run hydro-sediment models with a morphological factor. The principle is to apply a multiplicative factor for erosion and deposition processes estimated by a hydro-sediment model (Franz et al., 2017; Le Tu et al., 2019; Elmilady et al., 2020). Usually, this technic does not exceed 100 years. However, some studies used much larger factors (400 in Braat et al., 2017) to explore morphological evolution over longer time scales.

Because of the different time and space scales they deal with, these two types of models are not used for the same purposes (Joseph et al., 2016). The upscaling of coastal processes representation is the key to understand many depositional systems, but they are ruled by the interaction of many processes such as waves, river flows, tides and storm events. The predominance of a particular process is linked to the configuration of the coast and many places have been described as tide dominated coasts (Choi and Dalrymple, 2004; Tessier, 2012; Zhang et al., 2017). Long term deposits in this type of environment are not easily simulated, hydro-sediment models are not able to provide results over geological time scale. On the other hand, stratigraphic models cannot simulate the detailed highly variable tidal hydrodynamic processes. Here, we propose to combine sedimentology, physics, and numerical modelling to explore the influence of the paleoenvironmental evolution (defined as bathymetry and sea-level variations) on the distribution and characteristics of tidal currents. From a geological point of view, we aim to understand how tides impact sediment deposits distribution and how it changes with paleoenvironmental evolution (seafloor morphology, sea-level variations). However, it is a difficult challenge to address, as we have no direct data on hydrodynamic characteristics dating back more than 300 years.

The idea is to rebuild paleoenvironments and model the associated tide oscillations. Wells et al. (2007b; 2007a) used the model ICOM (Imperial College Ocean Modelling) during 30 days in order to study the tidal distribution during a high sea-level period (highstand) and an early stage of a transgression (late Pennsylvanian, 298.9 to 323.2 Ma). Tidal reconstructions at a global scale were also performed for the Aptian (125 Ma to 113 Ma, Wells et al., 2010). Those pioneering works led to many other studies to model the tide in the past with the model ICOM and even to correlate these simulations with sedimentary deposits by calculating the bed shear stress (Cretaceous, Bohemian basin, Mitchell et al., 2010; late Oligocene-Miocene, South China Sea, Collins et al., 2018). All those studies considered only the tide in hydrodynamic calculations. The approach proposed and the reconstructions provided by Imperial College are major advances in the understanding of the paleoenvironment influence on past tides and their subsequent impact on sedimentation at large spatial (sedimentary basin to global) and temporal (about 10–50 Myr) scales.

In this study, four paleoenvironments are generated to represent tidal evolution during Holocene period in the Bay of Brest (France). The paper is structured as follows. After introduction, section 2 (Study area context) describes the bay of Brest, its geological setting, our knowledge of the present-day hydrodynamic context and its Holocene history. Section 3 (Methods) describes the model used with its parametrization, the setting up of the scenarii and potential erosion and deposition indexes. Hydrodynamics influence on sedimentation evolution linked with the rise of sea-level and seafloor changes is detailed in section 4 (Results). These results are then discussed in section 5 and the main conclusions and perspectives are finally drawn up in section 6.

2. The study area: the bay of Brest

2.1. Geological description

The shape of the Bay of Brest is a consequence of three major orogenic episodes creating the Pentevrian (2 Ga to 750 Ma), Cadomian (600–530 Ma) and Hercynean (380–250 Ma) chains (Ballèvre et al., 2009, 2014). The Hercynian chain was divided into different provinces, separated from each other by faults and grinding zones. The North Armorican Shear crosses the study area and formed the bed of the Elorn river and the strait between Plouzané and the Roscanvel peninsula, named the "Goulet" (Fig. 1).

During the tertiary era the bay of Brest emerged several times, because of glacio-eustatic movements and the basement was eroded by paleo-rivers during low sea-level stages (Hallegouet et al., 1994). It resulted in three morphological domains (Figs. 1 and 2): T1 is the main channel, where paleo-rivers flowed; T2 consists of the first stage of terraces, above T1; T3 corresponds to the shallowest terraces close to the present-day shoreline, localized in sheltered coves and bays. A network of secondary channels within T2 and T3 connects these domains to the

main channel (T1). More details on the geomorphology of the bay of Brest are provided in Gregoire et al. (2016).

The 180 km^2 bay can be divided in two parts. The central part has its limits at two straits, the first formed between Plouzane and Roscanvel and the second between Lanveoc and Daoulas peninsula (Fig. 1). The upper part (can be named inner zone too) is at the east of the strait between Lanvéoc and Daoulas peninsula (Fig. 1). The outer zone corresponds to the Iroise sea and is not analysed in this study.

2.2. Hydrodynamic characteristic of the Bay of Brest

The bay of Brest is classified as a macrotidal system (Fig. 1). The mean spring tidal range is 5.9 m and the mean neap tidal range is 2.80 m in Brest harbour (Beudin, 2014). The Bay is protected from oceanic waves thanks to the strait between Plouzané and Roscanvel peninsula. This strait is 1.8 km wide connecting the Iroise sea and the bay of Brest. The semi-enclosed configuration of the bay of Brest induces a very weak swell climate compared to the energy regime outside the bay. Indeed, the swell is attenuated at the passage of the strait by the refraction on the edges and is diffracted at its exit. Thus, while the mean annual wave height is 2.4 m further offshore in the Iroise Sea, in the port of Brest, the mean annual significant wave height value is about 0.25 m (Monbet and Bassoullet, 1989). This statement is supported by the example of the Bella storm, which exposed the Iroise Sea to swells of almost 10 m and at the same time the bay of Brest suffered waves of less than 1 m (Fig. 3a and 3b). Under classic forcing (waves from WSW, max 3 m in the Iroise Sea and 33 km/h wind from the NE, Fig. 3c) the bay of Brest experiences waves around 0.22m (mean, Fig. 3d). In the latter case, the wave orientation in the bay clearly indicates that it is forced by the NE wind. Even if the wind sea takes over the ocean swell inside the bay, wind remains a minor forcing because of the short fetch of the bay of Brest (~25 km max, Stéphan et al., 2012). This particular configuration allows us to focus on the tidal dynamic.

2.3. Holocene history

During the last deglaciation, the sea-level rose quickly at the beginning of the Holocene in Brittany and gradually slowed down until it reaches today's level (Goslin et al., 2015). During the rise of sea-level in the bay of Brest, 4 sedimentary units were deposited: U0, U1, U2 and U3 (Gregoire, 2016). The Holocene story of the bay of Brest started with a mean sea-level 35 m lower than today. At this time (10 000 years ago) only the main channel was submerged (T1). Unit U0 was deposited at this time and was mainly composed of coarse continental sediments. Unfortunately, no samples could have been taken from this unit, so this interpretation relies only on seismic facies (Gregoire et al., 2017).

At 9000 years cal BP, sea-level reached −26 m from the present-day level, resulting in water submersion on T2 terraces (intertidal area, Fig. 5). This age marked the start of U1 deposition (Fig. 4). The sea-level rise was rapid during the deposition of U1 and at 7500 years cal BP, the sea-level exceeded the elevation of most of the T3 terraces, placing them in the intertidal area (Fig. 5). During the interval 9000–7000 years cal BP (Unit 1 deposition), most of deposits were muddy and preserved in the T3 domain. No deposit was preserved on T2 and only three patches were recorded in the main channel, two in the central part and the thinnest between Lanvéoc and Daoulas Peninsula (Gregoire et al., 2017, and Fig. 6 below).

The beginning of the U2 deposit was estimated at around 7000 years cal BP with a sea-level of −5 m relative to the present one (Figs. 4 and 5). The water level rose gradually over the interval 7000–3000 years cal BP until it reached the current sea-level. The MFS (Maximum Flooding Surface), set ~3000 years cal BP correspond thus to the top of the transgressive U2 (Fig. 6). U2 is interpreted as mainly cohesive sediments on T3 and sandy sediments in the main channel (Gregoire, 2016). No information is available for the sediment's nature present over few areas of T2.

The more recent sedimentary unit, U3, started ~2000 years cal BP and is still active now (Fig. 4). Deposits related to U3 take place over the MFS surface. They are present over all morphological domains and exceed 5 m in thickness only on rare occasions in the main channel and

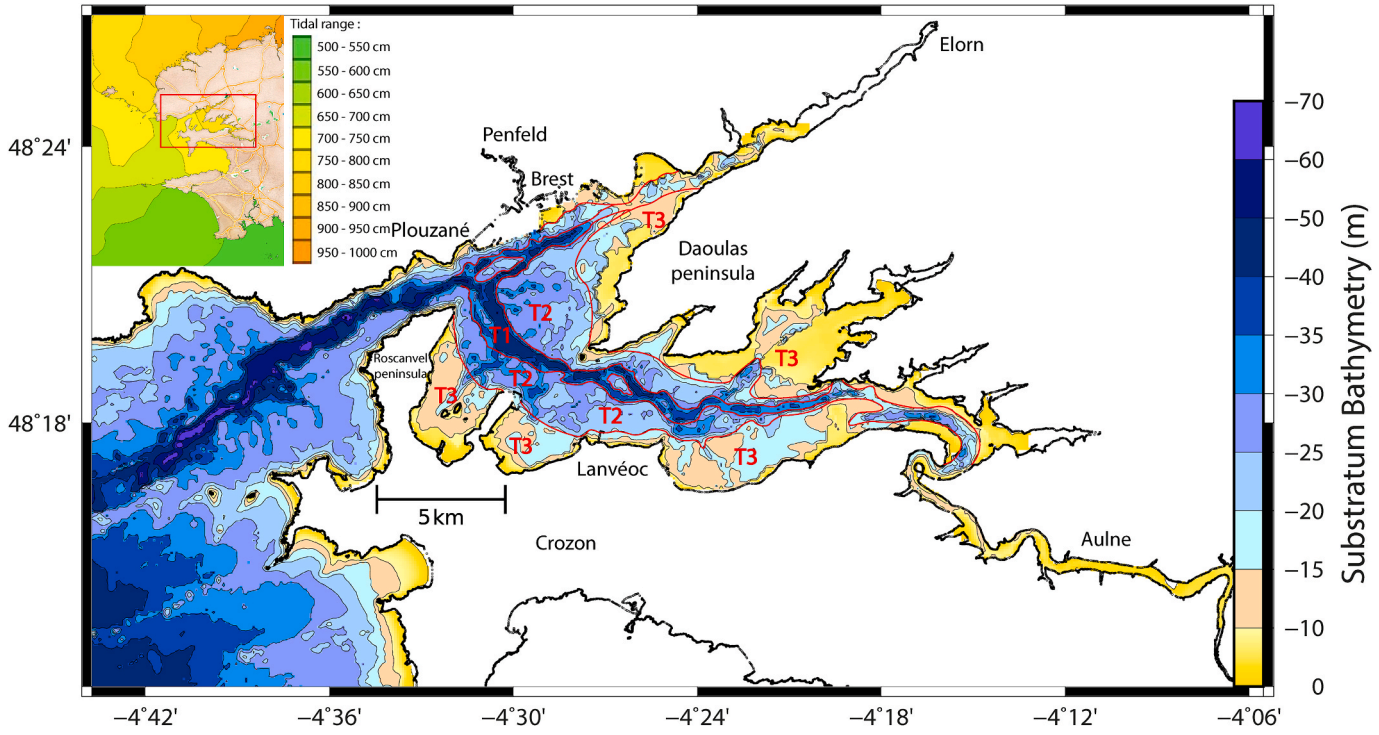

Fig. 1. Bathymetric map of the bay of Brest basement relative to the present-day mean sea-level. The inset-map, modified from SHOM (2015a), shows the tidal range of an exceptional spring tide (tidal range between 7.5 and 8 m). T1: main channel. T2: first terraces stage. T3: the shallowest terraces.

on T2 terraces (Fig. 6). The map of the present-day sedimentary cover of the bay of Brest (Gregoire, 2016) shows coarse sands and gravels over T2 at the north of the central area of the bay and sands at the south. The main channel shows all sizes of sand and the T3 terraces mainly mud. The upper zone is composed of finer sediments, described as a mixture of sand and mud.

3. Methodology and tools

The challenge is to rebuild key stages of the paleoenvironmental evolution and run hydrodynamical simulations with the resulting past bathymetries to explore the associated hydrodynamics and its impact on sediment distribution. First, the model and its setup are described in part 3.1. Then, the chosen periods that represent the key steps of the paleoenvironmental Holocene evolution of the study area are presented (part 3.2). The method to rebuild these paleoenvironments (each defined by their specific bathymetry and sea-level) is explained in part 3.3. Finally, a potential erosion and a potential deposition index are proposed to help correlation between sediment deposits and simulated bottom currents (see 3.4).

3.1. The hydrodynamic model (MARS3D)

The code used for this study is the model of coastal hydrodynamics MARS3D (Lazure and Dumas, 2008). It is a finite-difference 3D code that computes tide propagation and associated currents from the resolution of the primitive equations using the hydrostatic equilibrium hypothesis and Boussinesq approximation. It is written in spherical coordinates for the horizontal and sigma coordinates for the vertical.

The Bay of Brest configuration for the present-day is issued by Petton (Pers. Comm). A horizontal Cartesian mesh of 250 m × 250 m is used. We assume some uncertainties in the geological data, in particular linked to sea-level variations, seismic interpretation and seismic covering (Goslin et al., 2015; Gregoire, 2016). A grid finer than 250 m would not be justified compared to our data set and their uncertainties. We look only at major hydrodynamic patterns and finer mesh size is not needed. The water column is vertically discretized into 20 levels to simulate properly the bottom currents (useful in the potential erosion and potential deposition indexes computation, see section 3.4).

The bed roughness distribution is taken uniform over the entire area. Indeed, since the sediment cover is unknown for the past stages in the Bay of Brest, the choice of a uniform roughness length helps not to produce misleading circulation with a badly validated parameterization and facilitate the comparison between the scenarii. It is set constant and equal to 3.35 mm from the Nikuradse formulation using an average grain diameter of 500 μm, which corresponds to the present-day observations and past stage (cores observations from Gregoire, 2016).

The simulations are run with realistic tides over the year 2014 for each selected combination of bathymetry and sea-level. The choice of the year 2014 is motivated by the availability of the validation (tidal gauge, 5 ADCP) and input data (river discharge, tidal spectrum) for that period.

The hydrodynamic circulation model is forced at the western and southern marine boundaries by the entire tidal spectrum (143 components) extracted from the SHOM CST-France (Le Roy, R., Simon, B., 2003), for each stage simulated. To study tidal currents over paleoenvironments the spectrum could be simplified, however the present-day configuration of the Bay of Brest used in other studies is already validated with the full spectrum only. The tide is very well described around Brittany at present time (atlas of 143 components). However, few data are available for different sea-level around Brittany and especially in the past. Previous works explored the possible effects on some tidal components of a higher sea-level (M2, S2, N2, M4, MS4 and MN4, Idier et al., 2017) and of a lower sea-level (M2, Uehara et al., 2006; Ward et al., 2016 and paleo-tidal ranges, Goslin et al., 2015). The simulations at large scale of Uehara et al. (2006) and Ward et al. (2016) explore the evolution of the M2 component of the tidal spectrum over the last 16 and 21 thousand years in the northwest European shelf seas. The M2 elevation amplitudes calculated in Ward et al. (2016) are equal at 0 ka and at 8 ka (between 2 and 2.5m, Beudin, 2014; Ward et al., 2016). Goslin et al., 2015 also show an equivalent tidal range between the present-day and 6 Ka, for the Porsmilin site (7 km from the entrance of the bay). Ward et al. (2016) reveals that M2 elevation amplitude is about 0.5 m higher at 10 ka than at present-day, at the NE point of Brittany (about 15 km from the entrance of the Bay). A harmonic decomposition is performed for the bay of Brest and reveals that the M2 component dominates in the bay of Brest. Its amplitude is about two times higher than S2 (ellipsis available in supplementary material, and Beudin, 2014). Tidal component analysis is not developed in this study that focuses on the evolution of tidal currents distribution and its impact on the seafloor. Even if the harmonic decomposition analysis is not developed in this study, it allows to consider an equal forcing in all the scenarii (comprise between 9000 years cal BP and the present-day). M2 amplitude is under estimated by 0.25 m at 9000 years cal BP (mean between 8 and 10 ka), this is considered acceptable in comparison to other set-up hypothesis (uniform bed roughness, river discharges) and data uncertainties (seismic Gregoire, 2016, sea-level Goslin et al., 2015). Furthermore, Goslin et al., 2015 show a decrease in the tidal range at the entrance of the Bay of Brest of about 30 to 50 cm between 6 ka and 8 ka. Following those simulations the tide would be rather underestimated for the oldest scenario in this study.

The model is also forced by daily flows of the main rivers: Aulne, Elorn and Mignonne (mean flow in 2014: 30 m/s, 10 m/s, 1.5 m/s). The real flow for the year 2014 is used thanks to the data of the DREAL Bretagne (Regional Directorate for the Environment, Planning and Housing, http://www.hydro.eaufrance.fr/).

This configuration of the bay of Brest was validated and used in other studies (Klouch et al., 2016; Frère et al., 2017; Petton et al., 2020) and also compared to various datasets (temperature/salinity and ADCP, Petton et al., 2016, 2021). It has demonstrated its ability to reproduce the main characteristics of oceanic flows (tidal amplitude and phase, 3D currents). A further validation is available in the supplementary material of this paper. It concerns currents velocity compared to 5 ADCP (over October 2014 (Petton et al., 2016), and on July 16, 2014) and water height compared to Brest harbour's tidal gauge over the whole year 2014. The comparison to hydrodynamic data is possible only for

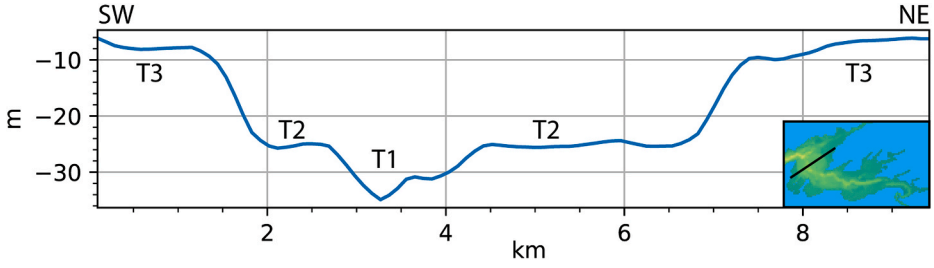

Fig. 2. Present-day bathymetric section relative to the present-day sea-level. T1: main channel. T2: first terraces stage. T3: the shallowest terraces.

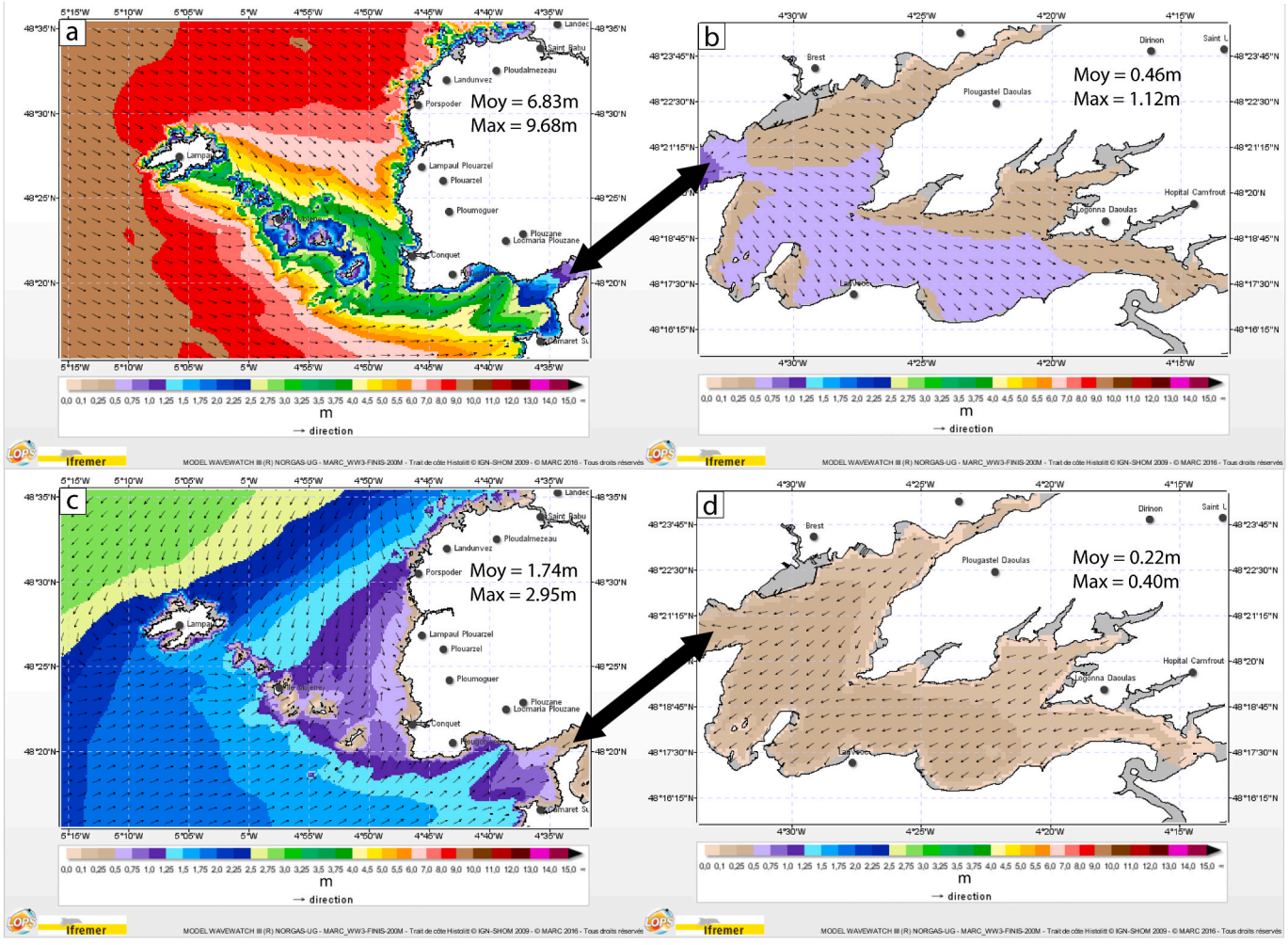

Fig. 3. Significant wave height in the Iroise Sea (a and c) and in the Bay of Brest (b and d). a and b are screen shot at 2 p.m. on 28/12/2020 during the Bella storm (wind: 40 km/h from NW, waves: from WSW). c and d are screen shot at 11 a.m. on 25/04/2021 (wind of 33 km/h from NE, waves from WSW), which represent a usual forcing over French Brittany coast. Data and illustrations from the ***marc*** operational forecast system (see website: http://marc.ifremer.fr/).

present-day, because of the lack of hydro dynamical data for the past.

3.2. Modelling scenarii

We generate a modelling scenario for each sedimentary unit, but U0 environmental context cannot be represented. We do not have enough information about it (no sample and no indication about the age of the layer base) and the mesh size of the grid (250 m) is often larger than the flooded area during this period. On the other hand, the immersion of the different morphological domains is an important paleoenvironmental change that must be simulated. Therefore, four scenarii are built corresponding to major paleoenvironmental changes between the periods of U1 (2 scenarii), U2 (1 scenario) and U3 (1 scenario) deposits.

The first scenario aims at reproducing the tidal dynamics at the beginning of U1 deposits. At this time (9000 years cal BP), the sea-level was −26 m below the present-day level. The bathymetry corresponds to the top of the U0 unit. T2 was in an intertidal domain and T1 was in a subtidal area (Fig. 5).

The objective of the second scenario is to model the final phase of U1 deposits, around 7500 years cal BP. The sea-level rose quickly at the beginning of the Holocene from −26m to −5 m. Due to these large sea-level variations, the context was very different throughout the deposit period of U1. In this second scenario, with a sea-level 10 m lower than the present-day, T3 was located in an intertidal area whereas T2 was in a subtidal area. As this scenario aims to represent the terminal deposits of U1 and the chronology of the deposits is unknown within 9 ka and 7 ka cal.BP (U1 deposit period), the input bathymetry chosen is the top of this same unit (Figs. 4 and 5).

The goal of the third simulation is to represent U2 deposit period. The third scenario was run at around 7000 years cal BP, with a sea-level at −5 m under the present-day level. Seafloor morphology at this time corresponded also to U1 top morphology. The sea-level rose only by 5 m during U2 period, and no major change was observed on the seismic data. So, only one scenario was built during the U2 deposit (Figs. 4 and 5).

The purpose of the fourth scenario is to reproduce the present-day context. The whole bay is submerged and mostly characterized by subtidal areas. The aim is to represent U3 dynamics which is still active at present day (Fig. 4).

3.3. Paleo-bathymetric reconstructions

The paleo-bathymetric reconstructions are based on seismic data collected during several cruises (see the complete list in Gregoire, 2016). The present-day depth of each seismic marker is calculated from the interpretation of the seismic data (Gregoire et al., 2017). Seismic depths in two-way travel time (seconds) is converted to depth (metres) by applying a constant velocity law in the sediment (1800 m/s) and in the water column (1550 m/s) to be consistent with previous studies (Gregoire et al., 2017). Bathymetric maps of the basement and thickness

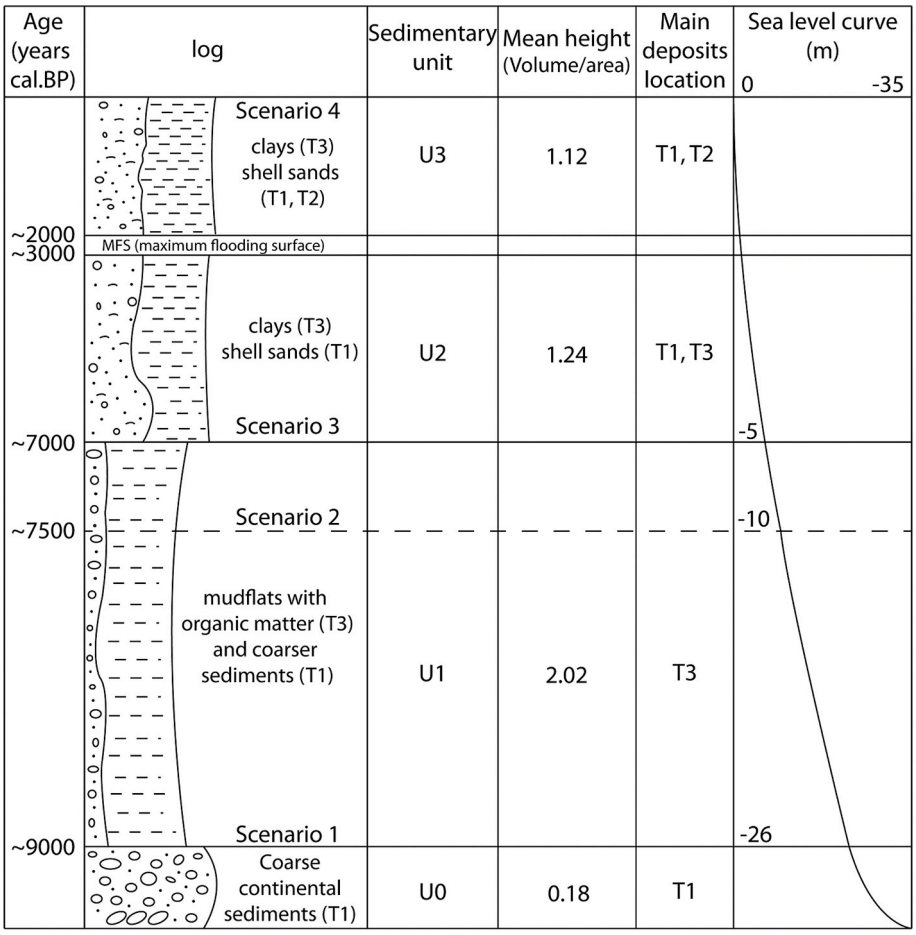

Fig. 4. Stratigraphic log of the Holocene period in the bay of Brest (modified from Gregoire, 2016). The vertical scale varies with the thickness of the units and the horizontal scale represents the global grain size of the units.

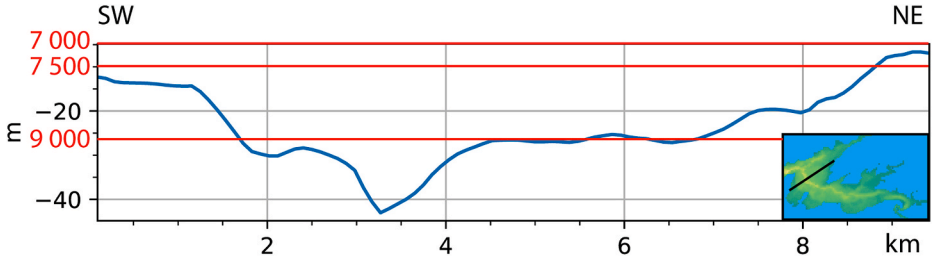

Fig. 5. Top U0 bathymetric section relative to the present-day mean sea-level. Red lines represent the mean sea-level at 9 000, 7500 and 7000 years cal BP.

maps of each unit were calculated with GMT (Generic Mapping Tool), using a 50 m spatial interpolation. The geological maps are finely meshed (50m) to prevent over-interpolation of sedimentary deposits. Wider interpolation would change the depositional boundary and the objective is to keep our validation data at the best possible resolution. These maps are then combined with the seabed present-day bathymetric data from the SHOM (2015b) to complete areas where no seismic data were available (the seismic data extension is available in Gregoire et al., 2017). Most of these areas are located in very shallow to intertidal areas, where no ship was able to perform seismic acquisition. So, they are emerged during all the scenarii except the present-day situation. This approximation has no influence on the simulated circulation in the bay of Brest, it is only performed for numerical purposes. Only in one place bathymetry is overestimated, because gas prevents a proper seismic acquisition and the sediment deposits could not be interpreted. It is located on T3 terraces at the south of the Daoulas peninsula, close to the mouth of the Mignonne River (Fig. 7).

U0 thickness is added to the basement map (Fig. 1) to generate seafloor bathymetry for scenario 1 (Fig. 7, Top U0). U1 thickness is added to the first scenario bathymetric map (U0 top, Fig. 7) and the result is the seafloor morphology for the second and third scenarii (Fig. 7, Top U1). The present-day morphological map is created from SHOM's data (Fig. 7, present-day bathymetry). The boundaries of the T1, T2, T3 domains (Fig. 1) are superimposed to each bathymetric map to allow us to see that these domains evolved slightly with sedimentary deposits, during the Holocene transgression.

3.4. Potential index calculation

Two different methodologies are used to observe the influence of simulated bottom currents on the seafloor. It seems important to separate sand and mud because of the different behaviour of these two types

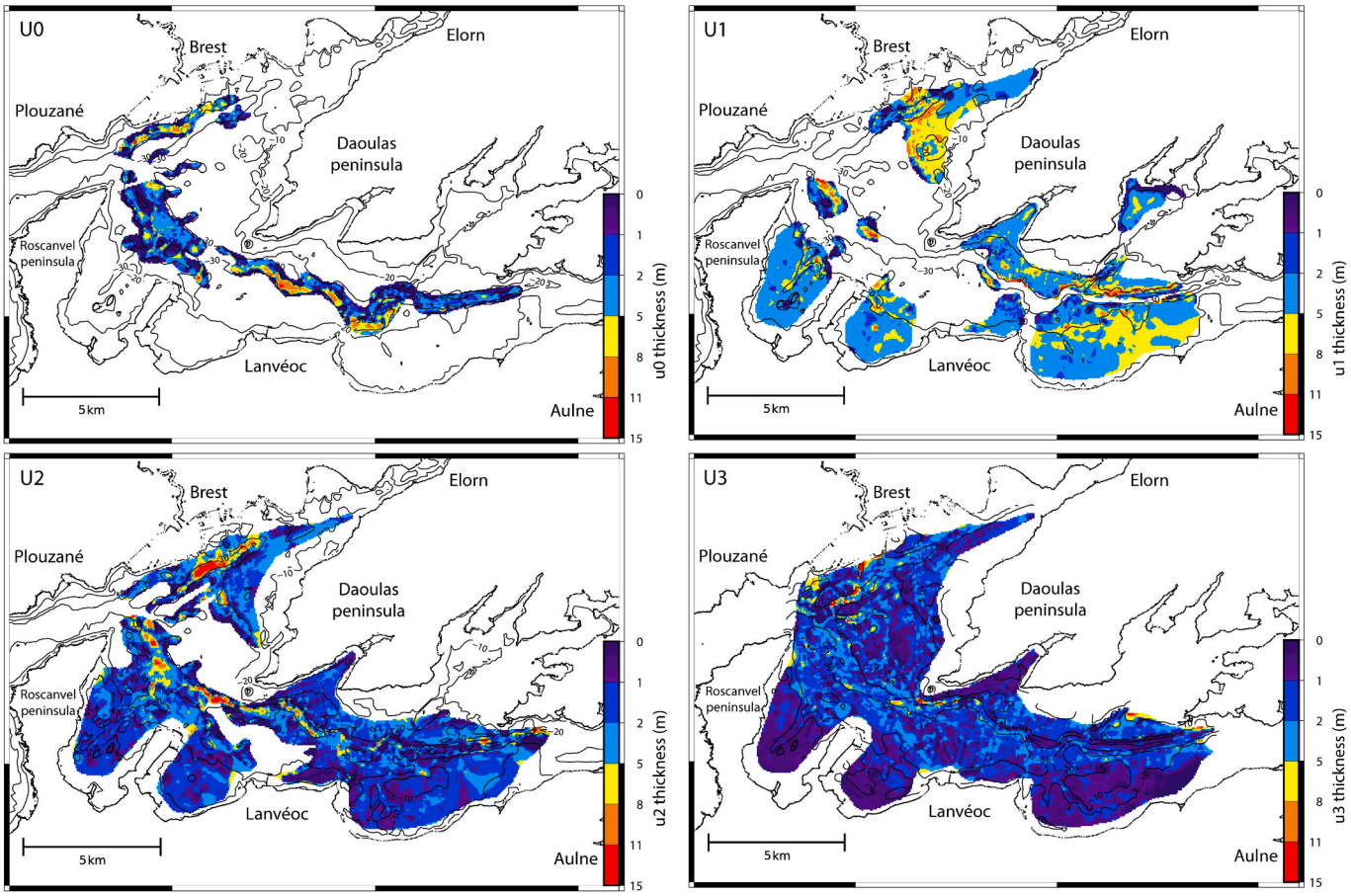

Fig. 6. Thickness maps of sedimentary units U0 to U3 (vertical seismic resolution around 1m) reconstructed with GMT from seismic interpretations of Gregoire (2016).

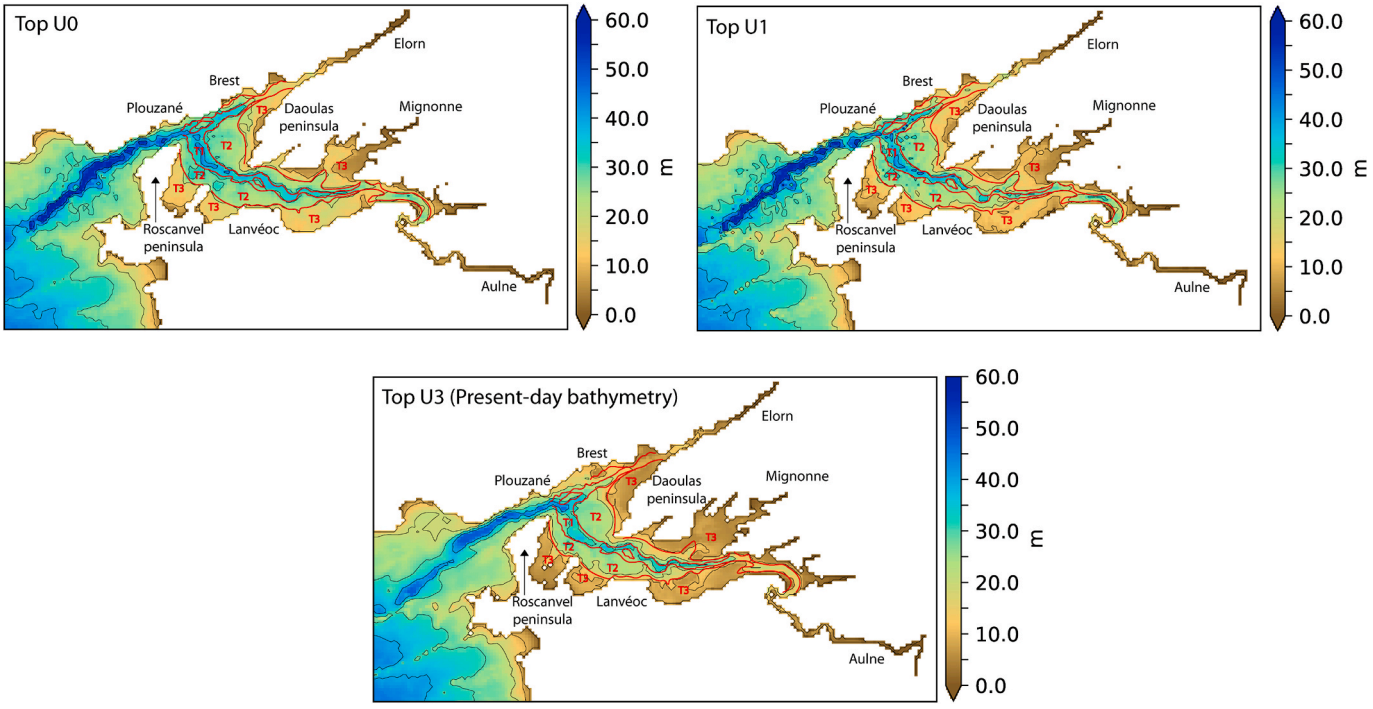

Fig. 7. Bathymetric maps of the top of U0, U1 and U3, relative to the present-day mean sea-level. Red lines represent the superimposed boundaries of the morphological domains of the basement map (Fig. 1).

of sediments. We perform an erosion potential index for non-cohesive sediments (see details below 3.4.1). As far as sands are concerned, most of the transport is realised by bedload or saltation (suspension phases are very short), so that no sand can be transported if there is no erosion zone nearby. It is therefore justified to look at potential erosion areas, which reveal the areas where non-cohesive sediments are potentially transported.

Fine particles can be transported in suspension for a long time, and their presence on the bed depends on the probability of deposition, more than on erosion possibility. This is especially true as deposited cohesive sediments are likely to be consolidated and hardly erodible after significant time. Thus, we calculated a potential deposition index (see details below 3.4.2) for cohesive sediments.

3.4.1. Potential erosion index

Non-cohesive sediments are characterized by a high settling rate and therefore settles right next to the areas where the stress is strong enough to trigger their reworking (depending on the size of the grain). To account for the variability of the stresses likely to displace a given sediment as a function of tidal range, Cognat (2019) proposed to calculate a potential erosion index that is characteristic of this grain size. This index is constructed as the integral over time of the a-dimensional shear excess. The a-dimensional shear excess is expressed as *F*. It stands for the excess of tidal current shear stress (τ_F) relative to the critical bed shear stress linked to the grain size classes of sediments (τ_c).

$$F = \int_t^n (f(t)) \tag{1}$$

With $f(t) = 0$ if $\tau_F(t) \leq \tau_c$

$$f(t) = \left(\frac{\tau_f(t)}{\tau_c}\right) - 1 \text{ if } \tau_F(t) > \tau_c$$

To determine the potential erosion index, it is therefore necessary to know the critical shear stress for each particle size class (τ_c) and the shear stress (τ_f) at each time step (Eq. (2)).

$$\tau_F(t) = \rho_{wat} * u^{*2}(t) \tag{2}$$

Where ρ_{wat} is the water density, fixed and equal to 1023 $kg.m^3$ and u^* is the friction velocity at t (Eq. (3)). The friction velocity is deduced from an assumed logarithmic velocity profile near the bed, and can be computed from the near bottom velocity provided by the numerical model and a skin roughness length *z0*.

$$U^* = \frac{K.U_{bot}(t)}{\ln\left(\frac{Z(t)}{Z0}\right)} \tag{3}$$

With *K* constant of Karman equal to 0.4, *z0* the skin roughness taken uniform and equal to 0.001 m. *z* represents the elevation where the bottom velocity U_{bot} is simulated, equal to the half of the bottom sigma layer. The critical shear stress (τ_c), needs to be determined for various granulometric classes. The grain size classes were estimated from previous work (Gregoire, 2016) and the study of about 10 core samples. Four sedimentary classes are selected D = 0,0030 m; 0,0011 m; 0,0002 m and 0,000015 m. For non-cohesive sediments, the critical shear stress (τ_c) for erosion is deduced from the Soulsby (1997) expression of the critical mobility parameter introduced by Shields (1936), based on experimental results. The mobility parameter θ represents the ratio between the flow-induced shear stress and the weight of sand particle in water:

$$\theta = \frac{u^{*2}}{(s-1)gD} = \frac{\tau}{\rho(s-1)gD} \tag{4}$$

Where *g* is gravity acceleration, *D* is the particle size, *s* the relative density of particles in water $s = \rho_{sediment}/\rho_{wat}$ and the critical mobility parameter of such particles is determined with Soulsby (1997) equation:

$$\theta_c = \frac{0.3}{1 + 1.2D^*} + 0.055[1 - \exp(-0.02D^*)] \tag{5}$$

where the non-dimensional diameter D* is deduced from the diameter D:

$$D^* = D\left[\frac{(s-1)g}{v^2}\right]^{\frac{1}{3}}$$

Where *v* is the kinematic viscosity of water.

Using equation (4), the critical shear stress is deduced from θ_c. The process is repeated for the three different particle sizes: D = 0,0030 m; 0,0011 m; 0,0002 m τ_c is calculated for each with Eq. (2) and the values obtained are presented in Table 1.

The potential erosion index F stands for the excess of bed shear stress compared to those values (τ_c, Table 1) and therefore represents the ability of tidal currents to rework and transport gravel, sand and fine sand from the seafloor.

3.4.2. Potential deposition index

The deposition potential index for cohesive sediments is based on a kind of "symmetric" concept. It represents the integral over time of the probability of mud deposition, following the concept introduced by Krone (1962): the (net) deposition rate of a cohesive sediment is proportional to the probability that a depositing sediment is not re-entrained by near-bottom turbulence, represented by the bed shear stress. Krone (1962) suggests a critical shear stress for mud deposition τd, above which deposition does not occur. The probability of deposition P(dep) reads:

P(dep) = 1-τ/τ_d, for $\tau < \tau_d$, and = 0 for $\tau > \tau_d$.

By this way, the potential deposition index can be computed for each mesh over the simulation (Eq. (7)).

$$F = \sum_{t=0}^{n} (f(t)) \tag{7}$$

With $f(t) = 0$ if $\tau_F(t) \geq \tau_d$

$$f(t) = \left(1 - \frac{\tau_f(t)}{\tau_d}\right) \text{ if } \tau_F(t) < \tau_c$$

According to literature, τ_d is in the order of 0.1 Pa for fresh (depositing) mud.

4. Results

All the results presented in this study intend to show the tidal currents distribution during the Holocene transgression. In order to discuss tidal impact on sediment movements, both depth-averaged velocity (4.1) and potential transport and deposition indices (4.2) are studied. The first subsection (4.1) aims to describe the ebb and flood tide barotropic currents. Currents directions evolution resulting from sea-level rise is analysed first. Then a percentile 90 is also calculated over one year to analyse the shift of the strongest ebb and flood barotropic currents between different scenarii and therefore try to interpret the evolution through time of the main likely sediment transfer zone within the Bay of Brest. The second subsection shows the potential erosion and deposition index calculated over one year. It allows to decipher where

Table 1
u_c^* and τ_c parameter for each grain size classes.

	Gravel 3 mm	Sand 1.1 mm	Fine sand 200 μm	Mud 15 μm (3.4.2)
u_c^* (Pa)	0.045	0.023	0.012	–
τ_c (Pa)	2.072	0.541	0.147	0.1

and how tidal near-bottom currents play and have played a major influence on the sedimentation/erosion couple (4.2).

4.1. Ebb and flood tide evolution

The results presented correspond to a mean over one flood and one ebb of maximum spring tides. We seek to highlight the changes in barotropic current directions between the different scenarii. Other analyses during neap or medium tides revealed similar directions with less intensity and a smaller spatial extension in general. Strongest currents (characterized by the largest spatial extension and the strongest velocities) will likely trigger much more (or of higher amplitudes) erosion or deposition processes. It is therefore more interesting to observe trends of a spring tide cycle.

During the first scenario (9000 years cal BP), ebb and flood tidal currents show the same patterns: they are confined in the deepest part of the bay in the main channel T1 (Figs. 8a and 9a). Ebb and flood display the same orientation and therefore currents are almost only bidirectional.

1500 years later, the sea-level has risen by 16 m, the flow of the ebb and flood tides is function of the coastline morphology. In the centre of the bay, straits (between Plouzané and Roscanvel peninsula and between Daoulas Peninsula and Lanvéoc) concentrate tidal energy and force the flood to flow through the north of the main channel and the ebb southwards of the central zone (Figs. 8b and 9b). In both cases, these water flows form an anticyclonic gyre, which is twice faster during flood than during ebb tide (Figs. 8b and 9b: 0.2–0.3 and 0.1 m/s respectively). The ebb and flood currents remain confined within the main channel in the upper zone of the Bay of Brest (upstream of the strait between Daoulas Peninsula and Lanvéoc), which is shallower than in the centre (T1 = 30–40m in the centre and 20–30m in the upper area). As T2 extension is smaller and smaller toward the Aulne mouth, T1 represents most of the subtidal domain in the upper area. The transition from the (very flat) T2 terraces into subtidal domain allows the tidal currents to extend over a much larger area. The new larger extension of T2 terraces permits the ebb and flood currents to propagate over different locations in the central zone (flood tide over T2 at the north and ebb tide over T2 and T1 at south) and form structures like the gyres.

In the third scenario (7000 years cal BP), ebb and flood directions are similar to scenario 2 in the centre of the Bay. The gyre grows in the centre and shows higher velocity during flood tide (0.3 m/s, for the southern part of the gyre, Fig. 8c). The major changes occur in the upper part: water flows are no longer confined within T1 domain after the strait between Daoulas Peninsula and Lanvéoc (Figs. 8c and 9c). Here T3 is located in the subtidal area, which allows ebb tide currents to expand over the entire upper zone. Orientation of the flood is triggered by the strait morphology between Lanvéoc and Daoulas peninsula and keeps a spatial distribution mostly over T1 and T2. Ebb and flood current propagate over different locations in the upper zone: flood tide flows to the East over T1 and T2 and Ebb tide flows to the West all over the area. This is due to the same process as the one observed in the centre of the bay during the scenario 2: an initial flat and large intertidal domain (around 2 and 3 km for terraces in the Bay of Brest) becomes the shallowest subtidal domain.

In the fourth scenario (present-day), ebb and flood tides directions and distributions are similar to those simulated in scenario 3. The size of the gyre at flood tide and the associated velocity are higher than in the previous context (0.3–0.4 m/s, for the southern part of the gyre, Fig. 8d). The gyre at flood tide becomes progressively wider and faster during the Holocene. Besides, the size of the gyre of ebb tide evolves very little during the same period and remains conversely slow. The increasing depth over the terraces allows to demarcate ebb and flood tides current distribution. Ebb tide shows similar vectors over the entire upper zone (Fig. 9d) while flood direction remains to the East, mainly localized over T1, oriented by the strait between Daoulas peninsula and Lanvéoc (Fig. 8, 9d). Even if the water depth has increased by 5 m compared to the previous scenario, the submerged area is almost identical. This leads to greater flooding upstream (higher tidal flow) and stronger tidal

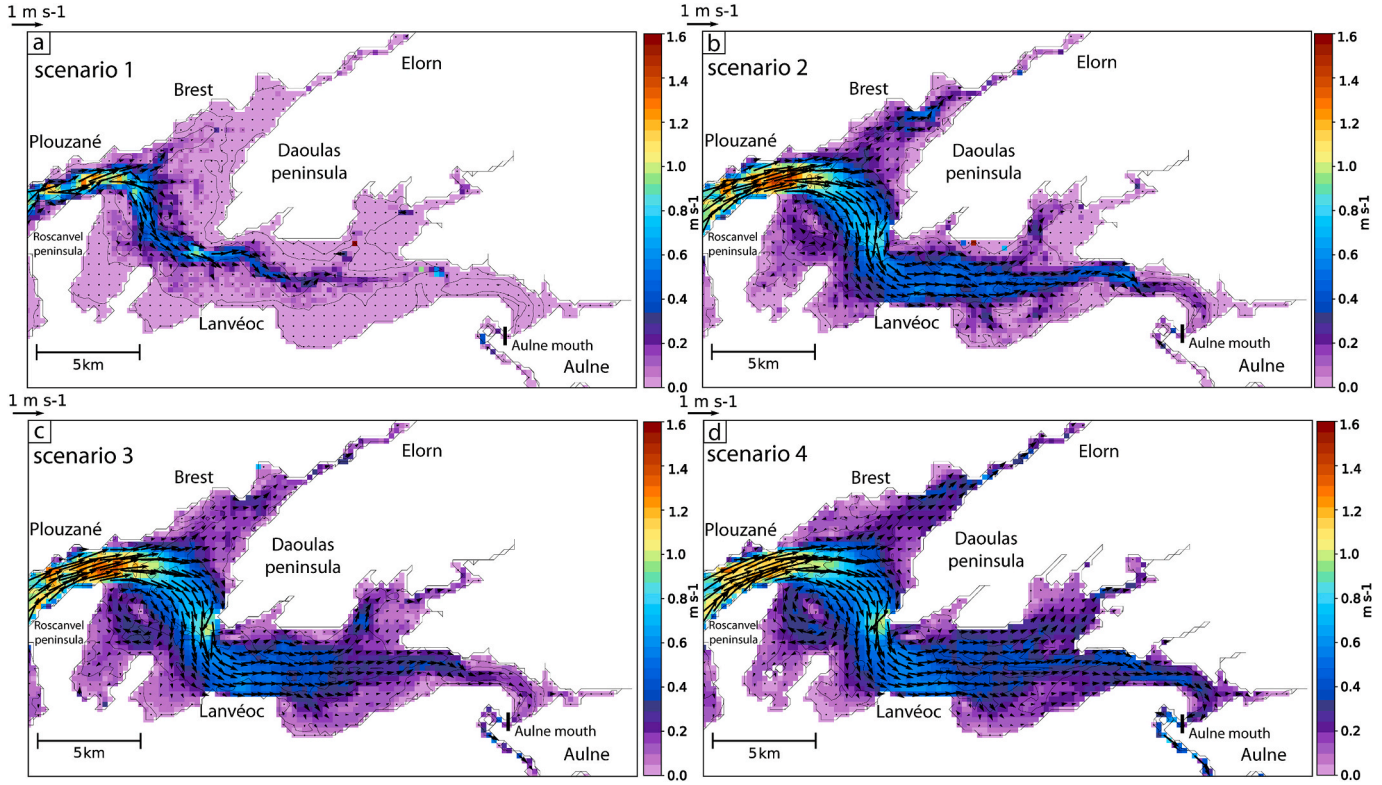

Fig. 8. Mean velocity and direction of tidal currents over one flood of maximum spring tide. a: scenario 1 (beginning of U1 deposits); b: scenario 2 (end of U1 deposits); c: scenario3 (beginning of U2 deposits); d: scenario 4 (top U3, still active).

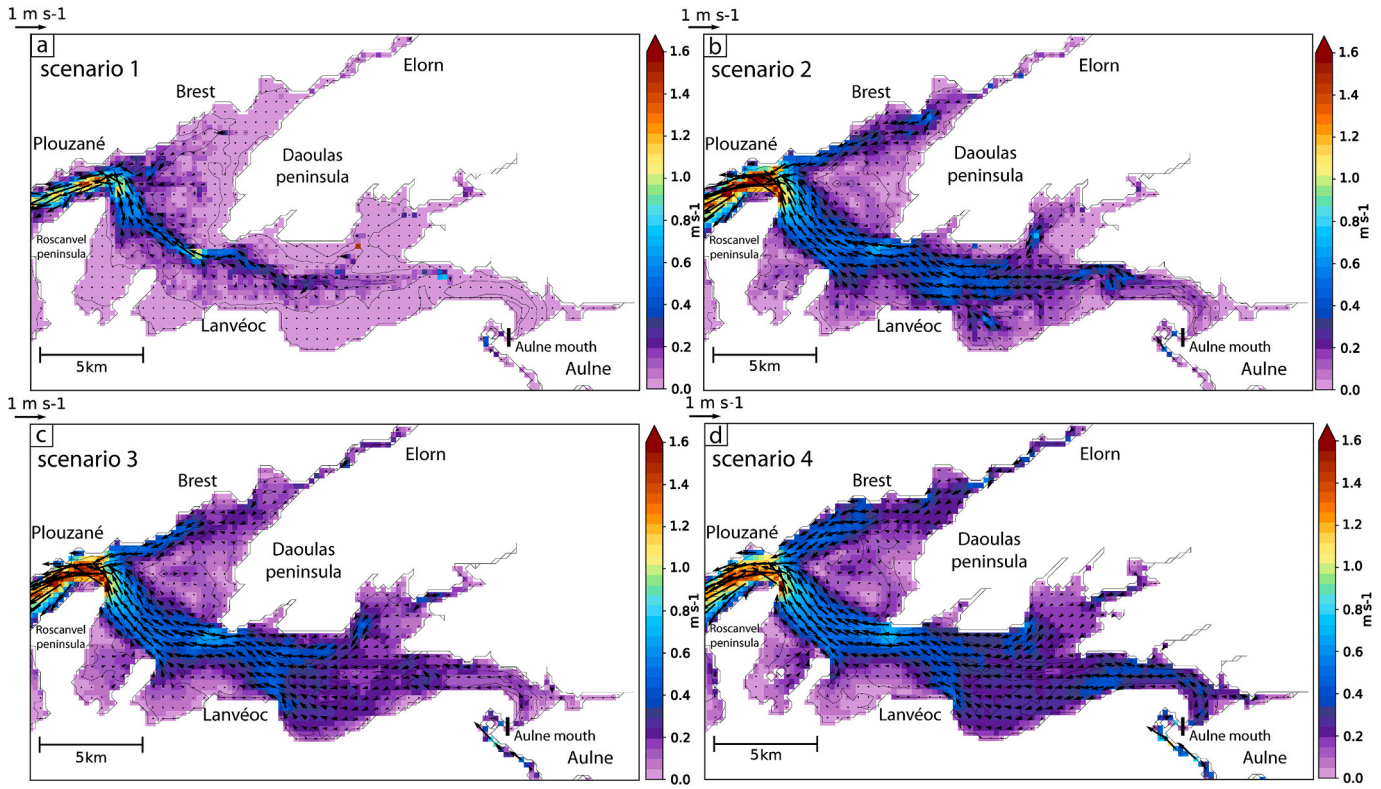

Fig. 9. Mean velocity and direction of tidal currents over one ebb of maximum spring tide. a: scenario 1 (beginning of U1 deposits); b: scenario 2 (end of U1 deposits); c: scenario3 (beginning of U2 deposits); d: scenario 4 (top U3, still active).

currents further upstream towards the Aulne and the Elorn rivers than in the previous scenario (Figs. 8d and 9d).

An analysis of currents direction during the river flooding event in February 2014 is performed to check if rivers flows may have also influenced these patterns. We try to quantify how far the Aulne river flow influenced the oscillating velocity signal corresponding to the tide from the river mouth (Figs. 8 and 9). This flooding occurred during neap and mid-tide cycles. The Aulne water discharge induces a downstream flow during flood tide 9 km downstream of the river mouth in scenario 1 and 11 km upstream during scenario 4 (Figs. 8 and 9). The present-day Aulne river flow is approximately three times stronger than the Elorn one. We thus infer that, as even a mega flood does not seem to compete with tide imprints (*a fortiori* during neap or middle tide), the rivers influence on the hydrodynamics inside the bay are weak compared to tidal impacts.

In order to understand the evolution of the areas under the influence of high barotropic ebb and flood tides, the 90 percentile is computed for each of them and for each scenario. The 90 percentile helps to look at the tidal current's maximum extent over the entire simulation and enables to remove potential excessive values. The objective is to identify the major changes in potential sediment transfer zones, with the analyse of the evolution of strongest currents over morphological domains between scenarii.

In scenario 1 (9000 years cal BP), the strongest currents (0.6 to more than 1 m/s) are located over T1. Ebb and food tides currents are located in the same places (Figs. 10a and 10b). Therefore, suspended matter transfer likely occurs mainly over T1.

In scenario 2 (7500 years cal BP), strongest currents (0.4–0.8 m/s, less strong than previously) extend to T2 in the centre of the Bay. Strong flood tide currents are visible over the entire T2 terraces with higher velocity at the north of the main channel (Fig. 10d). Strong ebb tide currents are observed south of the central zone over T1 and T2 (0.4–0.8 m/s, Fig. 10c). Most of the potential suspended sediment transport therefore shifts from T1 in scenario 1 to T2 in scenario 2. Upstream of the strait between Daoulas Peninsula and Lanvéoc, strongest velocities of ebb and flood tides are mainly localized over T1 and in secondary channels that connect T3 and T1 (0.4–0.7 m/s, Fig. 10c and 10d).

In scenario 3 (7000 years cal BP), the locations of high intensity of ebb and flood tides areas are similar to those of the previous scenario (0.4–0.8 m/s, in the centre of the bay), but their extents are slightly larger (Fig. 10e and 10f). The biggest changes occur in the upper area: the flood velocity decreases on T1 compared to scenario 2 (0.3–0.4 m/s, Fig. 10f) and the ebb tide is faster on T3 than on T1 (0.25 m/s and less than 0.2 m/s, Fig. 10e).

In scenario 4 (present-day), ebb and flood display the same pattern as in the 2 previous scenarii in the central part (0.4–0.8 m/s, Fig. 10). Between Brest and Daoulas peninsula over all the T3 terraces ebb and flood velocity is around 0.2 m/s (Fig. 10g and 10h). In the upper part, T3 terraces are mostly affected by ebb, but with higher currents (0.3 m/s, Fig. 10g). Strong currents are simulated more upstream toward the Aulne river than in scenario 3 (0.4–0.6 m/s, Fig. 10g and 10h). The present-day context presents the highest potential transport for suspended sediments over T3 (Fig. 10). Only the two terraces located at the south of the central zone, between Roscanvel peninsula and Lanvéoc are less impacted by tidal flows, because they are protected by the coastline (Fig. 10).

These percentiles and currents directions reveal an evolution of the location of main tidal currents: (1) They are confined in the main channel (T1) with high velocities during ebb and flood tides (section 4.1.2) and opposite directions (section 4.1.1). (2) As soon as the area surrounding T1 becomes subtidal (T2 at 7500 years cal BP in the central zone and T3 at 7000 years cal BP in the upper zone), velocities decrease within the main channel and strongest currents spread over the domain surrounding T1 (section 4.2.2). The sea-level rise over a terrace strongly increases the submerged area (due to a very flat morphology). This leads to a differentiation between ebb and flood tide current distribution, which is mainly influenced by straits morphology (section 4.1.1). It is the strait between Lanvéoc and Daoulas that leads the ebb over T1 in the

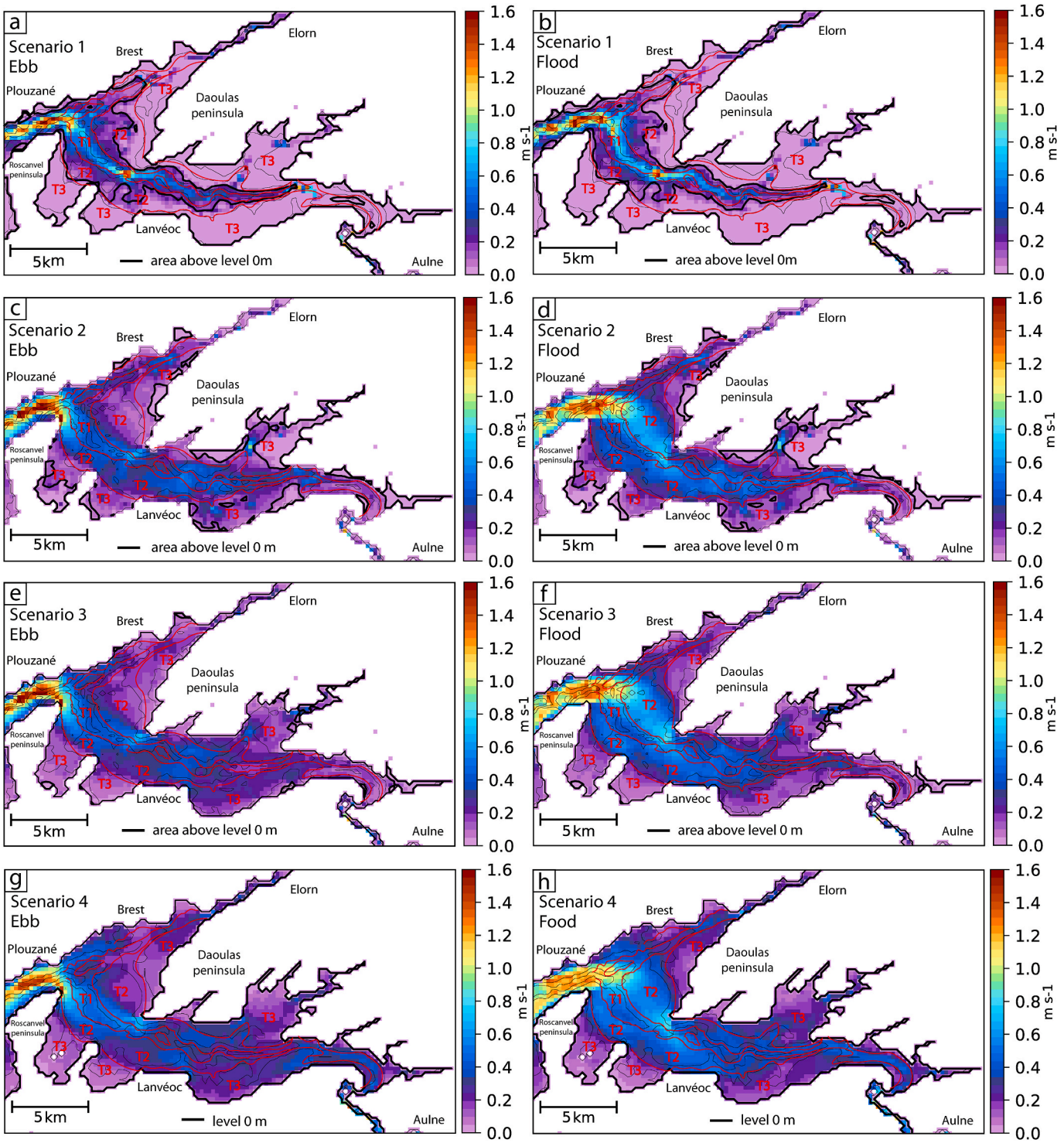

Fig. 10. Percentiles 90 of barotropic currents over one year, for ebb (a, c, e, g) and flood (b, d, f, h) tides during each scenario. The level 0m represents the mean sea-level of the scenario and red lines are the limits of the morphological domains.

central zone and the flood over T1 in the upper zone. Another effect of the strait influence is that currents are always eastwards at north of the central zone and always westward at the south. (3) The submerged area between scenario 2 (7500 years cal BP) and 3 (7000 years cal BP) increases a lot with the passage in subtidal domain of most of the T3 terraces, while sea-level increases by 5 m. Currents spread over a much larger area in the estuary and less intense currents than before reach the upper zone (section 4.2.2). The submerged area between scenarii 3 (7000 years cal BP) and 4 (present-day) is almost the same, most of the T3 terraces are already in subtidal domain in scenario 3 and the sea-level increases by 5 m. The inundation upstream increases and strong tidal current spread further upstream into the estuary in scenario 4 than in scenario 3 (section 4.2.2).

Changes in tidal current intensity are mainly related to the increase of the basin width in relation to the water height. Higher velocities are observed in the upper part of the estuary when the sea-level increases and not the submerged surface; and weaker velocities are observed upstream when the submerged surface increases and not the sea-level.

4.2. Bottom currents impact on the seafloor

This section aims to explore the influence of tidal bottom currents on the seabed which means on the erosion/deposition patterns via the analysis of a potential erosion index for non-cohesive sediments and a potential deposition index for cohesive sediments (section 3.4). Those indexes help to make the link between the simulated currents and the sediment records, by estimating the potential loss or deposition of sediment induced by bottom tidal currents over one year.

In the first scenario (bathymetry at the top of U0 and sea-level at −26 m relative to present-day), all grain size classes present a high erosion potential in the main channel, except gravels which are only mobilisable in the narrowest parts of the channel (Fig. 11). The intertidal zone (T2 domain) shows a much lower erosion index (Fig. 11b, c, 11d) and the highest potential deposit for mud (Fig. 11a). The T2 terraces may receive most of the cohesive sediment deposits (mud) and some fine sand.

In the second scenario (bathymetry at the top of U1 and sea-level at −10 m relative to present-day) the erosion potential index is the highest over T2 domain in the centre of the Bay of Brest. The action of the currents on the bottom is less intense in T1 than in the previous scenario (Figs. 11 and 12) and the T2 domain displays currents able to carry sands and fine sands (Fig. 12b and 12c). The deepest part of T1 and on slopes between T2 and T3 become the most favourable areas for the deposition of sands and fine sands. The maximum potential deposit for mud is located over T3 terraces (Fig. 12a). Over T1 in the upper part of the Bay of Brest, fine sands potential erosion is similar as over T2 in the centre and is strong in secondary channels too (Fig. 12b). Fine sands are therefore transported to T2 and T3 in the upper zone.

In the third scenario (bathymetry at the top of U1 and sea-level at −5 m relative to present-day), the centre of the Bay of Brest displays a similar potential erosion and deposition as in the second scenario, but the area with highest erosion potential is more extended at the south of the centre of the bay (Fig. 12b, 12c, 13b, 13c). The potential deposition of mud is the highest over T3 in the central zone (Fig. 13a). In the upper zone, in the main channel (T1) the potential erosion index for fine sands is tenfold lower than in scenario 2 (Figs. 12b and 13b). The distribution of the potential deposition for mud also highlights a decrease in bottom current velocity, which is greater on T1 and more uniform throughout the upper zone than in the previous scenario (Figs. 12a and 13a).

During the scenario 4 (present-day bathymetry and sea-level), the areas of potential erosion of all grain size classes cover a larger area and show a similar intensity than the previous scenario (Fig. 13b, 13c, 13d, 14b, 14c, 14d). The deepest zones (T1) are still less affected by potential erosion than in the T2 terraces in the centre. The potential deposition of mud displays the highest values over T3, but these values decrease over T3 in the upper zone compared to scenario 3 (Figs. 13a and 14a). New areas of strong bottom action appear near the river mouths in this scenario (Aulne and Elorn). In those areas the potential mud deposit is equivalent as in the centre (around 10^3, Fig. 14a) and even sands can be mobilized close to the Aulne river mouth (Fig. 14c).

The estimates of potential erosion and deposition indexes allow us to correlate major trends between simulated hydrodynamics and sediment records. The erosion potential indexes are first mostly localized in the main channel, then with sea-level rise, the high erosion potential extends to T2 domain in the centre of the Bay (between scenario 1 and 2, Figs. 11 and 12). In the same time strong potential deposition index for mud moves from T2 to T3, when T3 are intertidal terraces (scenario 2). All the muds deposited over T2 in scenario 1, are removed during scenario 2 and settle over T3. This is consistent with the deposition of U1, with only a few accumulations in the main channel in the centre of the Bay and most of the preserved sediments are observed on T3 domain (Fig. 6). Then, during scenario 3 bottom currents display similar patterns in the central zone, with a higher ability to carry non-cohesive sediment at the south (Figs. 13a and 13b). Between scenarii 2 and 3 (Figs. 12 and 13), the values of potential erosion decrease within the main channel in the upper area. Upstream of the strait between Daoulas Peninsula and Lanvéoc, the potential deposition of mud increases over T1 between scenario 2 and 3, and during U2 deposits are observed over all the upper zone. Only T2 at the north of the main channel in the centre and between Daoulas peninsula and Lanvéoc is under erosion (Fig. 6). During scenario 4, potential mud deposition decreases over T3 in the upper zone

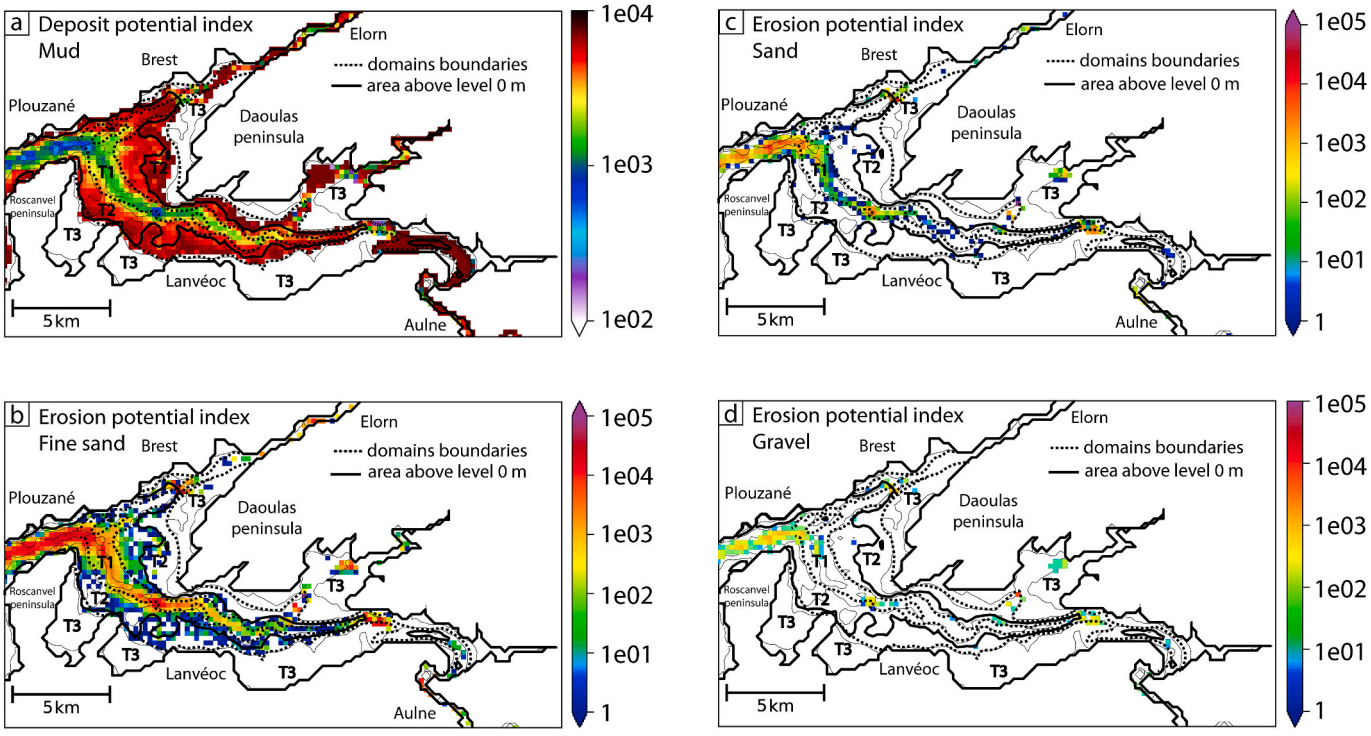

Fig. 11. Deposition potential (a: mud) and erosion potential indexes (b: fine sands, c: sands, d: gravels) calculated for scenario 1 (beginning of U1 deposits). Black lines represent the area above the mean sea-level and white zones are equal to 0.

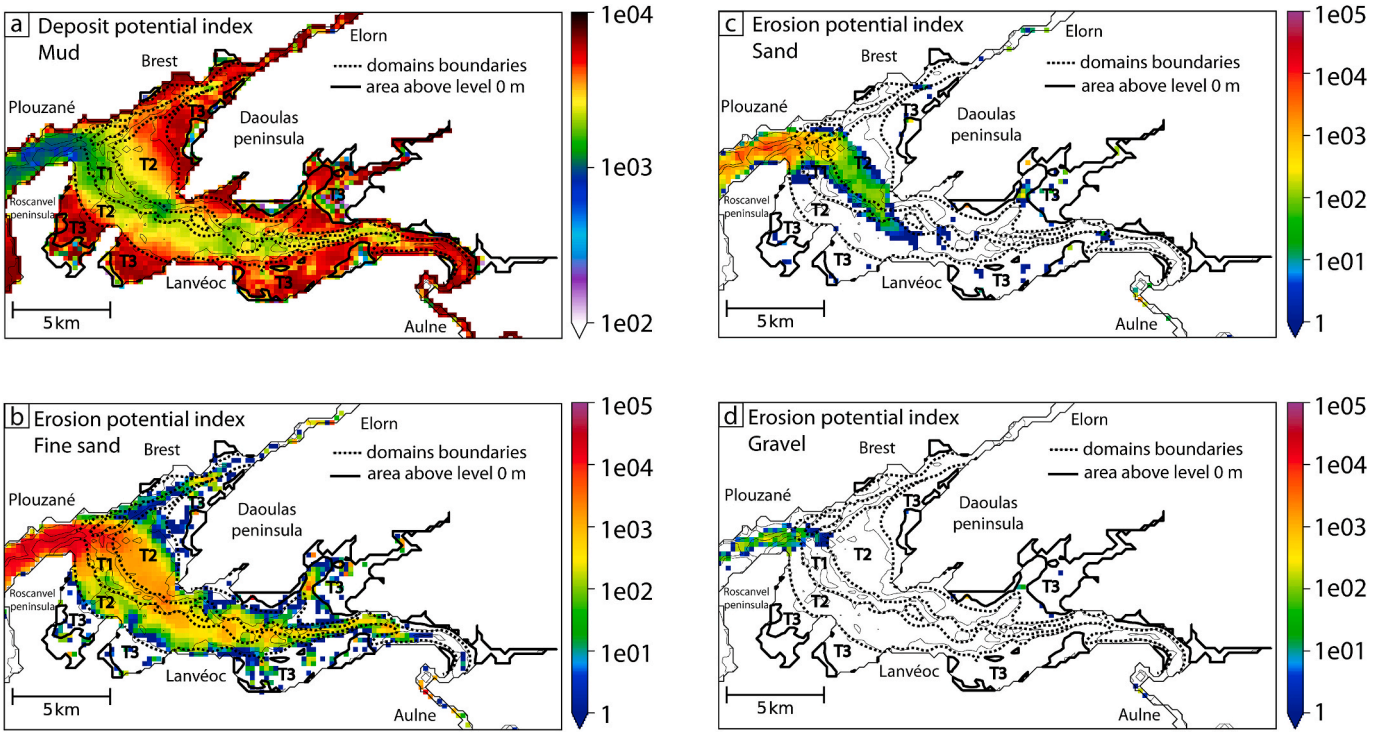

Fig. 12. Deposition potential (a: mud) and erosion potential indexes (b: fine sands, c: sands, d: gravels) calculated for scenario 2 (end of U1 deposits). Black lines represent the area above the mean sea-level and white zones are equal to 0.

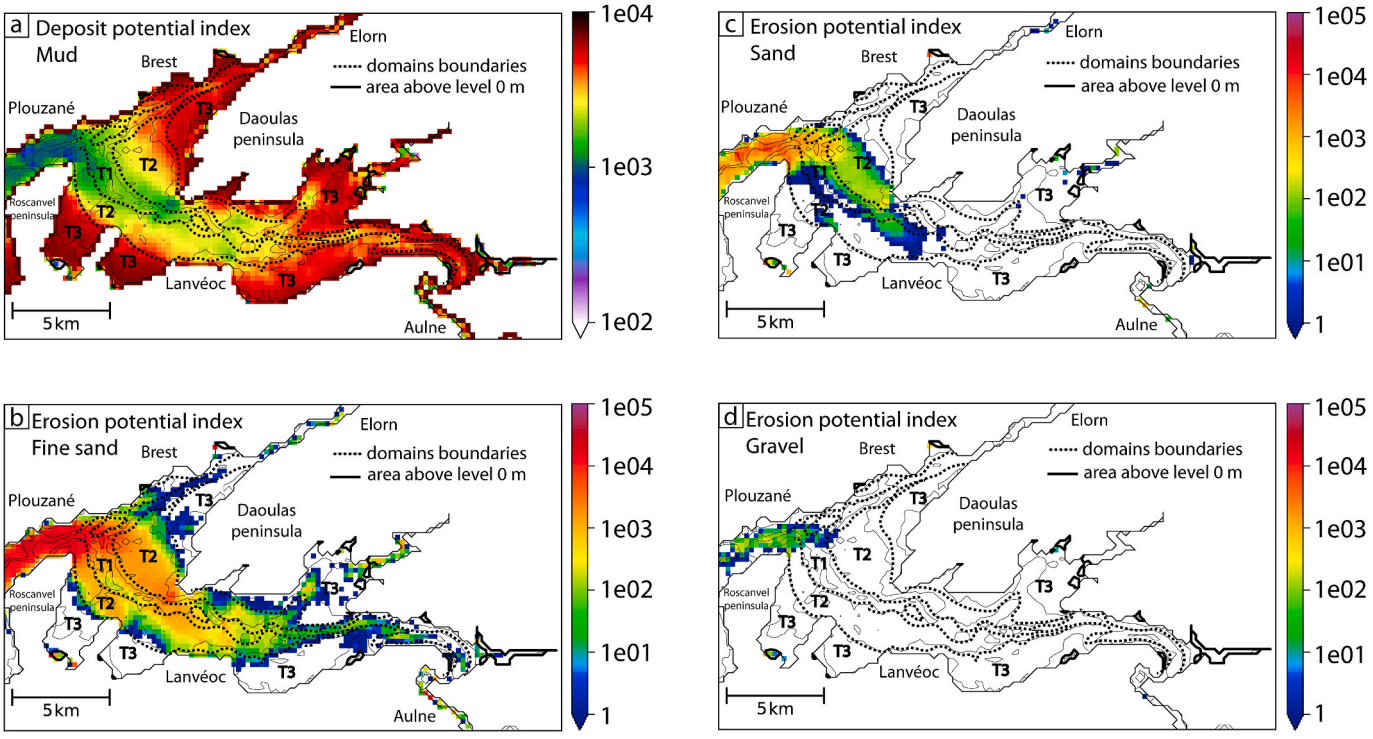

Fig. 13. Deposition potential (a: mud) and erosion potential indexes (b: fine sands, c: sands, d: gravels) calculated for scenario 3 (beginning of U2 deposits). Black lines represent the area above the mean sea-level and white zones are equal to 0.

compared to the previous scenario and potential erosion of fine sands shows that bottom currents are able to transport fine sands to or from the river mouths (Fig. 14b). In the centre of the Bay similar patterns are observed as in scenario 3. U3 thickness map shows the lowest thicknesses over T3 compared to U1 and U2 and important deposits over T1 (Fig. 6). That correspond to the potential erosion and deposition simulated, but several meters of U3 sediments are recorded over T2 in the central zone and remain unexplained (Fig. 6). The sedimentary map of Gregoire (2016) provides more information about the grain size classes repartitions for the present-day: (i) T2 is mainly covered by very coarse

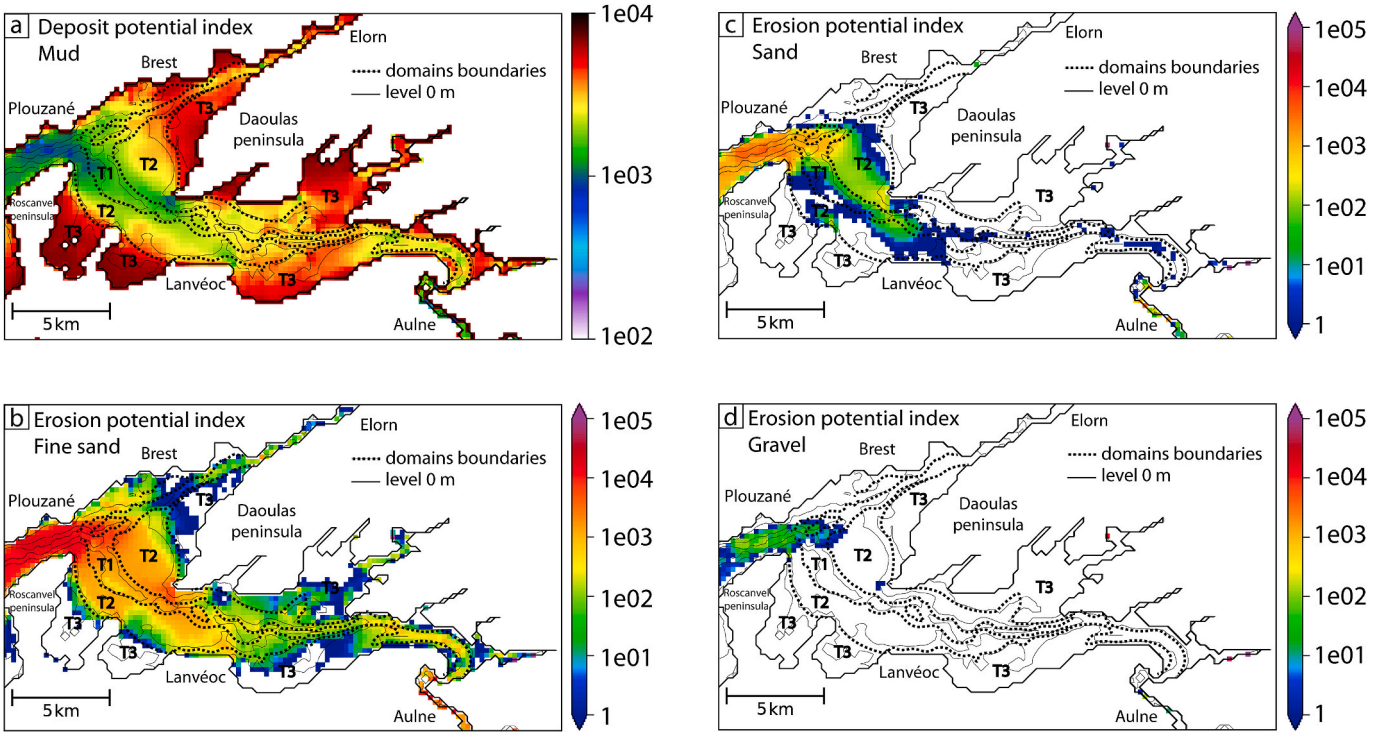

Fig. 14. Deposition potential (a: mud) and erosion potential indexes (b: fine sands, c: sands, d: gravels) calculated for scenario 4 (top of U3 deposits, still active). Black lines represent the mean sea-level and white zones are equal to 0.

non-cohesive sediments at the north of the main channel, (ii) sands and fine sands predominate at the south and within the main channel (T1), and (iii) muds are predominant over T3. (iiii) The surface coverage of the upper part is made mostly of cohesive sediments with a sandier mixture on T1 and T2 than T3. We simulate a similar repartition in the central part, with sands transport mostly at the north, fine sands that can be mobilized over T2 and T1 at the south of the central zone and strongest muds potential deposits over T3 (Fig. 14). In the upper area, the sediment map from Gregoire (2016) and the computed indexes show a good match too: potential deposition index for muds is higher over T3 than T1 and T2, and only fine sands are able to be transported by bottom currents in the upper area (mostly over T1 and T2, Figs. 14a and 14b).

In the centre, the hydrodynamic patterns remain similar since the scenario 2, strong currents over T2 transport cohesive sediments towards the shallowest morphological domain (T3, scenario 2, 3 and 4, section 4.1) and towards the remote and quiet zones of the estuary, both are the only places where muds display a strong potential deposition index (Figs. 12a, 13a and 14a). Potential erosion index indicates that non-cohesive sediments (except gravel) are presumed to be transported mostly over T2 in the centre and deposited in the main channel (T1) and on slopes between T2 and T3 (both located at the edges of T2 terraces, Figs. 12–14).

5. Discussion

In this study, we proposed paleotides reconstructions and discussed their impact on the distribution of the sedimentary units of the Bay of Brest, but some uncertainties need to be taken into account. To extend the bathymetric coverage on T3, at the south of the Daoulas peninsula, present-day bathymetric data were used. We do not know what is the effect of this overestimated bathymetry on the distribution of tidal currents in the upper zone. The ebb tide could have flowed over this part of T3 domain earlier than in scenario 3, depending on U2 and U3 thicknesses. The presence of Brest harbour also prevents a bathymetric reconstruction at the north of the central zone, because no records are available due to human modifications. In this area past hydrodynamics cannot be simulated correctly.

The choice to carry out a second scenario for U1 allows to highlight the influence of a significant coastline movement on the distribution of tidal currents. However, the true date of this paleoenvironment (T3 intertidal, scenario 2) is unknown, because the chronology of deposition within U1 is unknown too.

The composition of each paleoenvironment seafloor is unknown and for this reason the bed shear stress is kept uniform. This can change the currents velocities, but it has a very slight influence compare to bathymetric and sea-level evolution.

The rivers discharge evolution is the greatest uncertainty of the study even if the bay is affected by small rivers. In the absence of records for past stages, a true water discharge cannot be implemented. The use of a hydro-sediment model is the only way to calibrate rivers discharge with a sensitivity analysis, by comparing the sediment rate simulated and the one from each paleoenvironment over the estuary. This methodology can be supported by qualitative information from palynological studies (Fernane, 2014; Lambert, 2017).

Last incertitude is about the tidal amplitude during the first scenario. The amplitude of M2 component could be under estimated of about 0.25m in our study (Ward et al., 2016), with an M2 amplitude of about 2m in the bay of Brest at the present-day (Beudin, 2014). Or conversely the entire tidal range could be overestimated by 0.50 m or more (Goslin et al., 2015) The consideration of the evolution of forcing in the past represent a great difficulty as no data are available. The quantification of their respective influence on hydro-sediment dynamic is a perspective for a future work. A deeper analysis of forcings (especially rivers discharge and tide) can help to understand past interactions in estuaries and their impact on estuaries filling.

Our reconstructions focused on the distribution of sedimentary units U1, U2 and U3 in the Bay of Brest. At the beginning of U1's deposition (9000 years cal BP, sea-level −26m), the main channel (T1) concentrated the strongest currents, which prevented the deposition of cohesive sediments. Muds were directed towards the intertidal domain (T2)

whereas sands and fine sands were transported upstream and downstream by the alternating ebb and flood tides, eventually triggering sand bars. The rapid sea-level rise moved T2 terraces into subtidal domain and T3 into intertidal domain at 7500 years cal BP (sea-level −10m). The submerged area increased considerably, allowing tidal currents to extend to T2 domain in the central area. The straits (between Plouzané and Roscanvel peninsula, and between Daoulas peninsula and Lanvéoc) oriented ebb tide southward and flood tide northward in the central zone. High flood velocities in the entrance of the Bay of Brest induced an anti-cyclonic gyre in the centre of the bay, with higher velocities at the North than at the South of the main channel. In this configuration the sediments previously deposited on T2 were eroded and transferred on T3 terraces. Non-cohesive sediments were mainly transported on T2 and deposited at the edge of the T2 terraces (slopes between T2 and T3 and into the main channel T1). This change in currents distribution explained the absence of muddy sediment within U1 over T2 and their records over T3. In the upper zone, strong flood and ebb tide currents in the main channel prevented sediment deposition during all U1 deposit period.

Even if the sea-level rise slowed down during U2 deposits (Goslin et al., 2015), T3 terraces also became subtidal (sea-level -5m) at 7000 years cal BP. It marked the start of U2 deposits. The currents distribution remained similar to the second scenario in the centre, still influenced by the straits morphologies, but characterized by faster currents and greater extension over T2 than during the previous 7500–7000 years cal BP period. U2 sandy sediments settled within the main channel and on slopes between T2 and T3, whereas muddy sediment settled on T3. Ebb tide flowed over the whole area in the upper zone, while flood tide was orientated towards T1 and T2 by the strait separating the central and the upper part of the Bay of Brest. The T3 flooding considerably increased the area over which the tidal currents flow, while the sea-level raised only by 5 m. Slower currents reached the upper zone and permitted U2 sediments to settle over the whole upper zone. They contained mainly mud mixed with fine sands on T1 and T2.

Then, between 7000 years cal BP and the present-day the velocity of the sea-level rise decreased (globally) until it reached the present-day sea-level, while the submerged area did not increase. Currents during U3 were faster than during U2 and the flooding increased upstream in the estuary, towards the river mouths (Aulne and Elorn). Tidal currents were able to transport non-cohesive sediments more upstream in the estuary than the currents during U2 and prevented the deposition of muds close to river mouths (Aulne and Elorn). Muds settled upstream in the rivers and over T3 terraces in smaller quantity than before. The tidal dynamics remained similar as the previous unit during U3 in the central zone, but an important sediment thickness is present over T2 in the centre. U3 is still active at the present-day, so these deposits are potentially still moving such as sand dunes. This hypothesis suggests that non-cohesive sediments were deposited on T2 during the deposition of U1 and U2 but have been constantly recycled for the last 7500 years. This should be verified with bathymetric acquisition at regular time-intervals or high-resolution seismic acquisition.

Our approach focusing on a macrotidal bay (180 km^2) over 9000 years considers much smaller temporal and spatial scales than previous works from the Imperial college (Wells et al., 2007a, 2007b, 2010) and is under the action of less forcings: waves and wind are considered negligible compared to the tide (section 2.1.2, Fig. 3) over the entire timescale. Its paleoenvironmental evolution over the last 9000 years (bathymetry, Gregoire et al., 2017 and mean sea-level, Goslin et al., 2015), reveals that the fetch length (25 km today –Stéphan et al., 2012) is shorter at lower sea-levels than the present-day one and that the strait protecting the estuary from the swell is already formed during the Pliocene (5.3 Ma to 2.8 Ma, Hallegouet et al., 1994). In our study the simulated past hydrodynamics can be almost exclusively related to tide propagation. As the hydrodynamic is validated for the present-day stage, we have confidence in the hydrodynamics produced with the other bathymetries. The fact that the hydrodynamic results presented in this study explain the sedimentary distribution observed during the Holocene transgression, shows that the assumptions made in this study are justified.

We use here the same methodology as that proposed by Mitchell et al. (2010) and Collins et al. (2018): rebuild paleoenvironmental scenarii to study the evolution of tidal currents distribution in the past. In our case, the Bay of Brest over the last 9000 years is well-known, thanks to sedimentary records. We were able to simulate 4 distinct and successive contexts (sea-level and associated paleogeography) that are representative of all the major trends/steps of the Holocene history. This hypothesis that the 4 chosen scenarii (corresponding to 4 discontinuous steps) are indeed representing continuous hydrodynamic changes is a critical point, but allows us to discuss which factor(s) may trigger the major hydrodynamics changes observed in our simulations over the Holocene.

Simulating tide dynamics over time periods of at least 1 Ka remains a challenge for the oceanographic and geological communities that face a scale problem between their respective modelling tools (Joseph et al., 2016). Hydrodynamic models are able to simulate processes over time periods ranging from few-days to around 10 years. With a simplified integration of the processes, or the use of a morphological multiplicative factor this type of model can simulate over hundreds of years. For stratigraphic modelling the problem is to downscale calculation steps. Stratigraphic model consider only the resultant effect of all the processes using diffusive equations that apply at basins scale and allow simulations over much longer time period (hundreds of Ma) with longer time steps (1ka to 10 Ma, Ku Shafie and Madon, 2008, Burgess in Roberts, 2012). This kind of model does not allow to take into account a process oscillating as quickly as the tide. It would need to upscale the tidal calculation (no general or global effect is known over long periods) or to downscale the calculation of the other processes, which is not the objective of stratigraphic model.

The scenarii are for now the only way to reach time scales of geological interest (at least 1 ka to 10 ka) in the study of the impact of tidal currents on sediment distribution. Discussing the hydrodynamic evolution during the entire transgression in the Bay of Brest is a first step towards upscaling of the tidal impact on sediment. In the future, we plan to use these 4 scenarii, representing all sedimentary units and major coastline changes, to explore possible simplification for tidal currents calculations. The aim is to use representatives simplified tides as inputs for a stratigraphic model and thus simulate the whole period (9000 years cal BP.). Potential deposition and erosion indexes are an interesting approach, as they allow to integrate in the simulations the impact of bottom tidal currents on sediments, without smoothing the extreme events (e.g. spring and neap tides). This appears as a good way to bring together fine (hydrodynamic) and long (stratigraphic) time scales.

6. Conclusion

This study explored the responses of the Mars3D hydrodynamic model to four paleoenvironmental contexts chosen and rebuild during the Holocene transgression in the Bay of Brest (9000 years cal BP. to present). These four scenarii represent all the units defined from sediment records (Gregoire, 2016) and extrema of the paleoenvironmental changes defined as bathymetric and sea-level variations. Our use of process-based models of a well-known estuary over well constrained time period (9 ka-Holocene) is a rather new attempt to better understand the changes and behaviour of tidal processes through changing environments. It permits to link tidal currents evolution to paleoenvironmental changes between scenarii and therefore discuss what triggers the observed evolution. This new approach simulates the evolution of tidal dynamics over the last 9000 years and highlights the impact of morphology and water depth on the tidal currents, as well as probable influence of bottom currents on deposition of cohesive sediments and erosion/transport of non-cohesive sediments. Based on these correlations between sedimentary archive and simulated tidal currents, the

study proposes a reconstruction of the sedimentary filling during the entire Holocene transgression in the Bay of Brest.

This study succeeded to correlate the results of hydrodynamic simulations and sediment records in a qualitative way. Further modelling would be required using the hydro-sediment module e.g. MUSTANG (MUd and Sand TrAnsport modelliNG, Le Hir et al., 2011) coupled to MARS3D to simulate sediment dynamics correlate simulated scenarii and data in a quantitative way. This would provide further evidence of the relevance and effectiveness/weaknesses of the method presented here.

Declaration of competing interest

The authors declare that they have no known competing financial interests or personal relationships that could have appeared to influence the work reported in this paper.

Acknowledgements

This work was funded by IFREMER (Institut Français de Recherche pour l'Exploitation de la Mer) and IFPEN (Institut Français du Pétrole et Energies Nouvelles), through a PHD grant awarded to M. Olivier and prepared at EDSML Doctoral School at UBO (University of Brest) We would like to thank Romaric Verney, Francois Dufois, Benedicte Thouvenin, for their numerous advices and help (all from DYNECO/DHYSED laboratory – IFREMER). We would like to thank also Sébastien Petton (LPI laboratory - IFREMER) for all the work he carried out with the present-day configuration of the Bay of Brest. We would like to thank Bernadette Tessier (M2C laboratory – Caen University), Laure Simplet (LGS laboratory – IFREMER) and Nicolas Le Dantec (LGO laboratory – IUEM)for their follow-up on my PhD committee. The authors acknowledge the fruitful and constructive English editing advice and corrections by Alison Chalm. Special thanks to Pascal Le Roy (LGO laboratory – IUEM), Axel Ehrhold (LGS laboratory – IFREMER), Gwenael Jouet (LGS laboratory – IFREMER) for their long-term work in the Bay of Brest and the numerous cruises they carried out and the data set they made available to us. This work was more particularly based on Gwendoline Grégoire's PHD (now at Intechmer). We would like to thank the Beicip-Franlab for providing us with a free license to OpenFlow suite, that allowed us to explore the possibilities of stratigraphic models and their requirements to take into account the tide impact on sedimentation. The authors acknowledge the journal's editor Nandhini Kamaraj and Soumya Alby, and the anonymous reviewer, for their advice and comments on the manuscript which greatly improved its quality.

Appendix A. Supplementary data

Supplementary data to this article can be found online at https://doi.org/10.1016/j.csr.2021.104595.

References

Ballèvre, M., Bosse, V., Ducassou, C., Pitra, P., 2009. Palaeozoic history of the Armorican Massif: models for the tectonic evolution of the suture zones. Compt. Rendus Geosci. 341, 174–201. https://doi.org/10.1016/j.crte.2008.11.009.

Ballèvre, M., Martínez Catalán, J.R., López-Carmona, A., Pitra, P., Abati, J., Fernández, R.D., Ducassou, C., Arenas, R., Bosse, V., Castiñeiras, P., Fernández-Suárez, J., Gómez Barreiro, J., Paquette, J.L., Peucat, J.J., Poujol, M., Ruffet, G., Sánchez Martínez, S., 2014. Correlation of the nappe stack in the Ibero-Armorican arc across the Bay of Biscay: a joint French–Spanish project. Geological Society, London, Special Publications 405, 77–113. https://doi.org/10.1144/SP405.13.

Bárcena, J.F., García-Alba, J., García, A., Álvarez, C., 2016. Analysis of stratification patterns in river-influenced mesotidal and macrotidal estuaries using 3D hydrodynamic modelling and K-means clustering. Estuar. Coast Shelf Sci. 181, 1–13.

Beudin, A., 2014. Dynamique et échanges sédimentaires en rade de Brest impactés par l'invasion de crépidules, p. 224.

Braat, L., van Kessel, T., Leuven, J.R.F.W., Kleinhans, M.G., 2017. Effects of mud supply on large-scale estuary morphology and development over centuries to millennia. Earth Surf. Dynam. 5, 617–652. https://doi.org/10.5194/esurf-5-617-2017.

Bruneau, B., Chauveau, B., Baudin, F., Moretti, I., 2017. 3D stratigraphic forward numerical modelling approach for prediction of organic-rich deposits and their heterogeneities. Mar. Petrol. Geol. 82, 1–20. https://doi.org/10.1016/j.marpetgeo.2017.01.018.

Cayocca, F., 2000. Long-term morphological modeling of a tidal inlet: the Arcachon Basin, France. Coast Eng. 42, 115–142. https://doi.org/10.1016/S0378-3839(00)00053-3.

Choi, K.S., Dalrymple, R.W., 2004. Recurring tide-dominated sedimentation in Kyonggi Bay (west coast of Korea): similarity of tidal deposits in late Pleistocene and Holocene sequences. Mar. Geol. 212, 81–96. https://doi.org/10.1016/j.margeo.2004.07.008.

Cognat, M., 2019. Rôles des facteurs environnementaux et des interactions biomorphodynamiques sur l'évolution spatio-temporelle des herbiers de zostères dans une lagune mésotidale.

Collins, D.S., Avdis, A., Allison, P.A., Johnson, H.D., Hill, J., Piggott, M.D., 2018. Controls on tidal sedimentation and preservation: Insights from numerical tidal modelling in the late Oligocene-Miocene South China Sea, Southeast Asia. Sedimentology 65, 2468–2505. https://doi.org/10.1111/sed.12474.

Crombez, V., Rohais, S., Baudin, F., Chauveau, B., Euzen, T., Granjeon, D., 2017. Controlling factors on source rock development: implications from 3D stratigraphic modeling of Triassic deposits in the Western Canada Sedimentary Basin. Bull. Soc. Geol. Fr. 188, 7. https://doi.org/10.1051/bsgf/2017188.

Dalrymple, R., 2010. Tidal depositional systems. In: James, N.P., Dalrymple, R.W. (Eds.), Facies Models 4: St John's. Geological Association of Canada, pp. 201–231.

Elmilady, H., Wegen, M., Roelvink, D., Spek, A., 2020. Morphodynamic evolution of a Fringing Sandy Shoal: from tidal levees to Sea level rise. J. Geophys. Res.: Earth Surface 125.

Fernane, A., 2014. Reconstitution des fluctuations holocènes en relation avec les changements climatiques et l'antropisation sur les côtes bretonnes à partir de bio-indicateurs fossiles (chironomidés, pollen et foraminifères benthiques). Brest, p. 248.

Franz, G., Delpey, M.T., Brito, D., Pinto, L., Leitão, P., Neves, R., 2017. Modelling of sediment transport and morphological evolution under the combined action of waves and currents. Ocean Sci. 13.

Frère, L., Paul-Pont, I., Rinnert, E., Petton, S., Jaffré, J., Bihannic, I., Soudant, P., Lambert, C., Huvet, A., 2017. Influence of environmental and anthropogenic factors on the composition, concentration and spatial distribution of microplastics: a case study of the Bay of Brest (Brittany, France). Environmental pollution (Barking, Essex 225, 211–222. https://doi.org/10.1016/j.envpol.2017.03.023, 1987.

Goslin, J., van Vliet Lanoë, B., Spada, G., Bradley, S., Tarasov, L., Neill, S., Suanez, S., 2015. A new Holocene relative sea-level curve for western Brittany (France): Insights on isostatic dynamics along the Atlantic coasts of north-western Europe. Quat. Sci. Rev. 129, 341–365. https://doi.org/10.1016/j.quascirev.2015.10.029.

Granjeon, D., Joseph, P., 1999. Concepts and Applications of a 3d Multiple Lithology Diffusive Model in Stratigraphic Modeling. Society for Sedimentary Geology (SEPM) Special Publications N°62.

Grasso, F., Le Hir, P., 2019. Influence of morphological changes on suspended sediment dynamics in a macrotidal estuary: diachronic analysis in the Seine Estuary (France) from 1960 to 2010. Ocean Dynam. 69, 83–100.

Gregoire, G., 2016. Dynamique sédimentaire et évolution holocène d'un système macrotidal semi-fermé. l'exemple de la rade de Brest, Brest, p. 294.

Gregoire, G., Ehrhold, A., Le Roy, P., Jouet, G., Garlan, T., 2016. Modern morpho-sedimentological patterns in a tide-dominated estuary system: the Bay of Brest (west Britanny, France). J. Maps 12, 1152–1159. https://doi.org/10.1080/17445647.2016.1139514.

Gregoire, G., Le Roy, P., Ehrhold, A., Jouet, G., Garlan, T., 2017. Control factors of Holocene sedimentary infilling in a semi-closed tidal estuarine-like system: the bay of Brest (France). Mar. Geol. 385, 84–100. https://doi.org/10.1016/j.margeo.2016.11.005.

Hallegouet, B., Lozac'h, G., Vigouroux, F., 1994. Formation de la Rade de Brest. Atlas permanent de la mer et du littoral n°1, p. 21.

Idier, D., Paris, F., Le Cozannet, G., Boulahya, F., Dumas, F., 2017. Sea-level rise impacts on the tides of the European Shelf. Continent. Shelf Res. 137, 56–71. https://doi.org/10.1016/j.csr.2017.01.007.

Joseph, P., Teles, V., Weill, P., 2016. Modelling approaches in sedimentology: introduction to the thematic issue. Compt. Rendus Geosci. 348, 473–478. https://doi.org/10.1016/j.crte.2016.04.001.

Klouch, Z.K., Caradec, F., Plus, M., Hernández-Fariñas, T., Pineau-Guillou, L., Chapelle, A., Schmitt, S., Quéré, J., Guillou, L., Siano, R., 2016. Heterogeneous distribution in sediments and dispersal in waters of Alexandrium minutum in a semi-enclosed coastal ecosystem. Harmful Algae 60, 81–91. https://doi.org/10.1016/j.hal.2016.11.001.

Krone, R.B., 1962. Flume Estudies of the Transport of Sediment in Estuarial Shoaling Processes. University of California, Berkeley.

Ku Shafie, K.R., Madon, M., 2008. A review of stratigraphic simulation techniques and their applications in sequence stratigraphy and basin analysis. BGSM 54, 81–89. https://doi.org/10.7186/bgsm54200814.

Lambert, C., 2017. Signature paléoenvironnementale des séquences holocènes en Rade de Brest : forçages climatiques et anthropiques. Brest, p. 248.

Lazure, P., Dumas, F., 2008. An external–internal mode coupling for a 3D hydrodynamical model for applications at regional scale (MARS). Adv. Water Resour. 31, 233–250. https://doi.org/10.1016/j.advwatres.2007.06.010.

Le Hir, P., Cayocca, F., Waeles, B., 2011. Dynamics of sand and mud mixtures: a multiprocess-based modelling strategy. Continent. Shelf Res. 31, 135–149. https://doi.org/10.1016/j.csr.2010.12.009.

Le Roy, R., Simon, B., 2003. Réalisation et validation d'un modèle de marée en Manche et dans le Golfe de Gascogne(application à la réalisation d'un nouveau programme de réduction des sondages bathymétrique. Rapport technique Rapport n002/03.
Le Tu, X., Thanh, V.Q., Reyns, J., Van, S.P., Anh, D.T., Dang, T.D., Roelvink, D., 2019. Sediment transport and morphodynamical modeling on the estuaries and coastal zone of the Vietnamese Mekong Delta. Continent. Shelf Res. 186, 64–76. https://doi.org/10.1016/j.csr.2019.07.015.
Mitchell, A.J., Uličný, D., Hampson, G.J., Allison, P.A., Gorman, G.J., Piggott, M.D., Wells, M.R., Pain, C.C., 2010. Modelling tidal current-induced bed shear stress and palaeocirculation in an epicontinental seaway: the Bohemian Cretaceous Basin, Central Europe. Sedimentology 57, 359–388. https://doi.org/10.1111/j.1365-3091.2009.01082.x.
Monbet, Y., Bassoullet, P. 1989. Bilan des connaissances océanographiques en rade de Brest. Rapport CEA/IPSN, code DERO/EL 89-23.
Petton, S., Le Berre, D., Haurie, A., Pouvreau, S., 2016. HOMER Campaign : Mooring Time Series.
Petton, S., Le Roy, V., Bellec, G., Queau, I., Le Souchu, P., Pouvreau, S., 2021. Marine Environmental Station Database of Daoulas Bay.
Petton, S., Pouvreau, S., Dumas, F., 2020. Intensive use of Lagrangian trajectories to quantify coastal area dispersion. Ocean Dynam. 70, 541–559. https://doi.org/10.1007/s10236-019-01343-6.
Posamentier, H.W., Allen, G.P., 1993. Variability of the sequence stratigraphic model: effects of local basin factors. Sediment. Geol. 86, 91–109. https://doi.org/10.1016/0037-0738(93)90135-R.
Roberts, D.G., 2012. Regional Geology and Tectonics: Principles of Geologic Analysis. Elsevier Science & Technology Books, Amsterdam, Nederlands.
Roelvink, J.A., 2006. Coastal morphodynamic evolution techniques. Coast Eng. 53, 277–287.
Shields, A., 1936. Application of Similarity Principles and Turbulence Research to Bed-Load Movement. Hydrodynamics Laboratory, vol. 167. California Institute of Technology, p. 43.
Service Hydrographique Et Océanographique De La Marine SHOM, 2015a. Marnages sur les côtes françaises de La Manche et de l'Atlantique pour le coefficient 120.
Service Hydrographique Et Océanographique De La Marine SHOM, 2015b. MNT Bathymétrique de façade Atlantique (Projet Homonim).
Soulsby, R., 1997. Dynamics of Marine Sands. Thomas Telford Publications, p. 249.
Stéphan, P., Fichaut, B., Suanez, S., 2012. Les sillons de la rade de Brest et les marais maritimes associés. FRAC GPN, p. 137.
Tessier, B., 2012. Stratigraphy of tide-dominated estuaries. In: Davis, R.A., Dalrymple, R. W. (Eds.), Principles of Tidal Sedimentology. Springer Netherlands, Dordrecht, pp. 109–128.
Tosic, M., Martins, F., Lonin, S., Izquierdo, A., Restrepo, J.D., 2019. Hydrodynamic modelling of a polluted tropical bay_ Assessment of anthropogenic impacts on freshwater runoff and estuarine water renewal. J. Environ. Manag. 236, 695–714.
Uehara, K., Scourse, J.D., Horsburgh, K.J., Lambeck, K., Purcell, A.P., 2006. Tidal evolution of the northwest European shelf seas from the Last Glacial Maximum to the present. J. Geophys. Res. 111 https://doi.org/10.1029/2006JC003531.
Ward, S.L., Neill, S.P., Scourse, J.D., Bradley, S.L., Uehara, K., 2016. Sensitivity of palaeotidal models of the northwest European shelf seas to glacial isostatic adjustment since the Last Glacial Maximum. Quat. Sci. Rev. 151, 198–211. https://doi.org/10.1016/j.quascirev.2016.08.034.
Wells, M.R., Allison, P.A., Piggott, M.D., Gorman, G.J., Hampson, G.J., Pain, C.C., Fang, F., 2007a. Numerical modeling of tides in the late Pennsylvanian Midcontinent Seaway of North America with implications for Hydrography and Sedimentation. J. Sediment. Res. 77, 843–865. https://doi.org/10.2110/jsr.2007.075.
Wells, M.R., Allison, P.A., Piggott, M.D., Hampson, G.J., Pain, C.C., Gorman, G.J., 2010. Tidal modeling of an Ancient tide-dominated Seaway, Part 1: model validation and application to global early Cretaceous (Aptian) tides. J. Sediment. Res. 80, 393–410. https://doi.org/10.2110/jsr.2010.044.
Wells, M.R., Allison, P.A., Piggott, M.D., Pain, C.C., Hampson, G.J., Dodman, A., 2007b. Investigating tides in the early Pennsylvanian Seaway of NW Eurasia using the Imperial College Ocean model. Geological Association of Canada,St. John's, Newfoundland Special paper 48, 363–387.
Zhang, X., Dalrymple, R.W., Lin, C.M., 2017. Facies and stratigraphic architecture of the late Pleistocene to early Holocene tide-dominated paleo-Changjiang (Yangtze River) delta. GSA Bulletin 130, 455–483. https://doi.org/10.1130/B31663.1.